5-1997

Geological and Geophysical Character of the East China and Yellow Seas

John D. Milliman
Virginia Institute of Marine Science

Nicole D. Scott
Virginia Institute of Marine Science

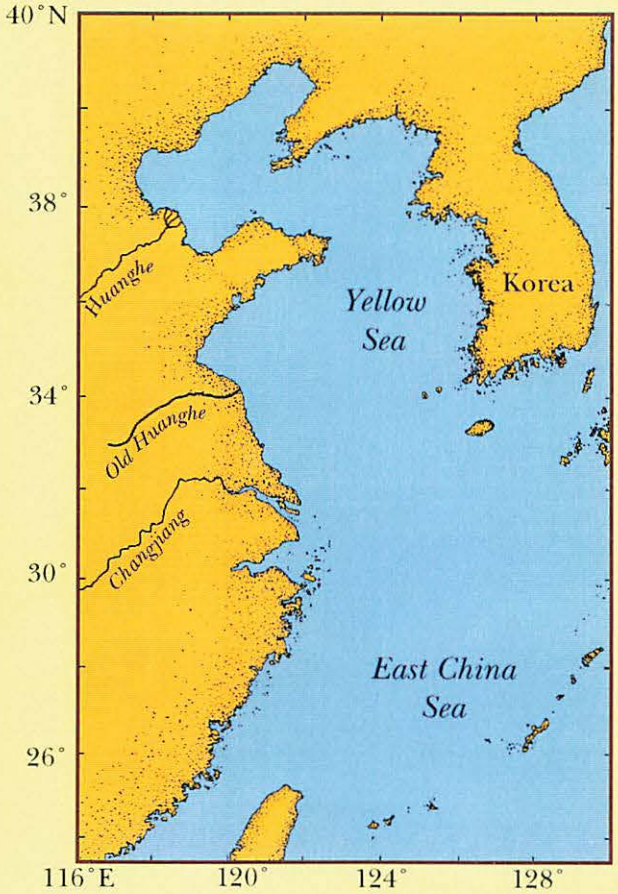

Geological and Geophysical Character of the East China and Yellow Seas

Prepared by
John D. Milliman and Nicole D. Scott

School of Marine Science
College of William and Mary
Gloucester Point, VA 23062

Prepared for
the NAVAL OCEANOGRAPHIC OFFICE (NAVOCEANO)

May 1997

Geological and Geophysical Character of the East China and Yellow Seas

John D. Milliman and Nicole D. Scott
School of Marine Science
College of William and Mary
Gloucester Pt, VA 23062 (804-642-7105)

Summary

The shallow (0-100 m) epicontinental Yellow and East China seas border the much deeper (depths locally exceeding 1000 m) Okinawa Trough. As a result oceanic currents in the area reflect both the influence land and the Kuroshio Current; the Taiwan Warm Water and Yellow Sea Warm Water currents both bringing clear warmer, saline waters from the Kuroshio, while the Changjiang Coastal Water, the Jiangsu Coastal Water and the Yellow Sea Cold Water transport turbid less saline waters to the south, particularly during winter Arctic-air outbreaks from northern China.

As a result of the regional circulation and the large sediment discharge from the Changjiang (Yangtze River) and Huanghe (Yellow River), the coastal area off China is dominated by thick deposits of Holocene muds. A band of Huanghe-derived muds extends down the central portion of the study area, south of Cheju Island. This mud patch is sandwiched on either side by relict sand patches. Because of the greater content of silt relative to clay, the Huanghe-derived muds along the Jiangsu coast and in the central areas have greater water contents, suggesting that objects placed on the seafloor in these areas would have a greater tendency to be buried.

Shallow biogenic gas is rare, occurring only in a few areas, most importantly in the thicker portions of the Shandong mudwedge, off the old Huanghe delta, and off the modern Changjiang river. No evidence of slope failure has been noted in either the Yellow Sea nor the East China Sea, although many examples of slope failure are seen in the Okinawa Trough area.

The deeper strata overlie a major seismic reflector, the strength of this reflector suggesting a much higher seismic velocity/impedance that the overlying section. Close correlation between the distribution and thickness of the overlying section on the one hand and a mosaic of published maps on the other indicate that these sediments are Neogene in age, having been deposited mostly in response to increased sediment supply due to uplift of the Himalayas. Subsequent regressions and transgressions of sea level, together with resultant low and high stands of sea level, have formed an alternating series of erosional and depositional sedimentary and acoustic facies, representing locally as many as five easily recognizable (on high-resolution seismic profiles) sea-level fluctuation events.

Although we have an excellent overall understanding of the marine geology and geophysics in the Yellow and East China seas, the lack of closely spaced both high-resolution and deeper seismic (particularly seismic refraction) data, prevents us from understanding geological conditions at

more local scales. Such data as well as direct access to the logs from deep borings, are needed if we are to understand local conditions and variations.

Table of Contents

	Page
Introduction	4
This Report	8
Regional Character	9
Bathymetry, Surficial Sediments, and Seafloor Morphology	11
Regional Oceanography	12
Modern Sediment Sources	17
Geotechnical Character of Surface Sediments	23
Late Quaternary/Holcoene Seismic and Sedimentologic Record	25
Buried Gas	29
The Neogene Record	36
Nature of the Deep Reflector	
Distribution of Sediments Overlying the Deep Reflector	
Geological Age and Significance of Sediments Overlying the Deep Reflector	
Unknowns and Future Studies	46
References Cited	47

Introduction

The East China and Yellow seas represent one of the broadest shallow seas in the global ocean, with water depths generally less than 80 m and stretching nearly 750 km from the Shandong Peninsula to the Okinawa Trough (Fig. 1). This area is also unique in terms of the vast amount of sediment it receives from the Huanghe (Yellow River; presently discharging in the adjacent Gulf of Bohai) and the Changjigang (Yangtze River, which flows into the East China Sea). Together, this region receives about ten percent of the river-derived sediment reaching the ocean, and as such, the region has unique geological and oceanographic conditions that reflect both the present highstand of sea level as well as previous lowstands.

The purpose of this report is to present and discuss the nature of the seafloor as well as the shallow structure of the surficial (Neogene) strata in the YS-ECS. The maps accompanying this report are the products of the analysis and interpretation of many types of seismic reflection data as well as many previously published papers dealing with this area. Specifically, we have utilized 3.5 kHz echo-soundings, various types of shallow-towed boomer profiles, sparker, air-gun and water-gun data as well as multichannel deep seismic data obtained by the former Gulf Oil Company. Moreover, we have integrated seismic refraction data gathered in the 1960's and 1970's (Fig. 2) in an attempt to gain better knowledge about the acoustic and (thereby) geological character of the deeper Neogene strata.

Unfortunately, the quality and nature of the geophysical data vary widely. The pioneering work by Emery in the late 1960's used sparker data recorded on 4-sec sweeps. As a result the data can best depict the depth to and configuration of the acoustic basement on a broad, regional basis; they do not have sufficient vertical resolution to portray anything concerning the Holocene, nor can they show local variations. A more extensive data set was collected by the first author as part of a cooperative study between the Woods Hole Oceanographic Institution and the Institute of Oceanology, Academia Sinica, Qingdao, from 1983-1986. These included side-scan sonar, 3.5 kHz echo-soundings, very high-resolution (Huntec DTS - resolution <0.5 msec), high-resolution (Geopulse) and deep (air gun) seismic data. As a result, there is a broad range in the resolution and penetration of the seismic profiles, from the meter-scale in the late Holocene to the 100's of m penetration to acoustic basement.

Available seismic refraction data are limited to sonobuoy studies made in the 1960's and early 1970's by the (then) Lamont-Doherty Geological Observatory (Murauchi et al., 1968; Leyden et al., 1973; Ludwig et al., 1973). Unfortunately, these data are restricted to the southern edge of the East China Sea and the adjacent Okinawa Trough. The present writers know of no seismic refraction data from the central East China Sea nor from the Yellow Sea. Statements regarding the seismic character of the seafloor sediments and deeper strata, therefore, must be made from geological inferences based primarily on seismic reflection data.

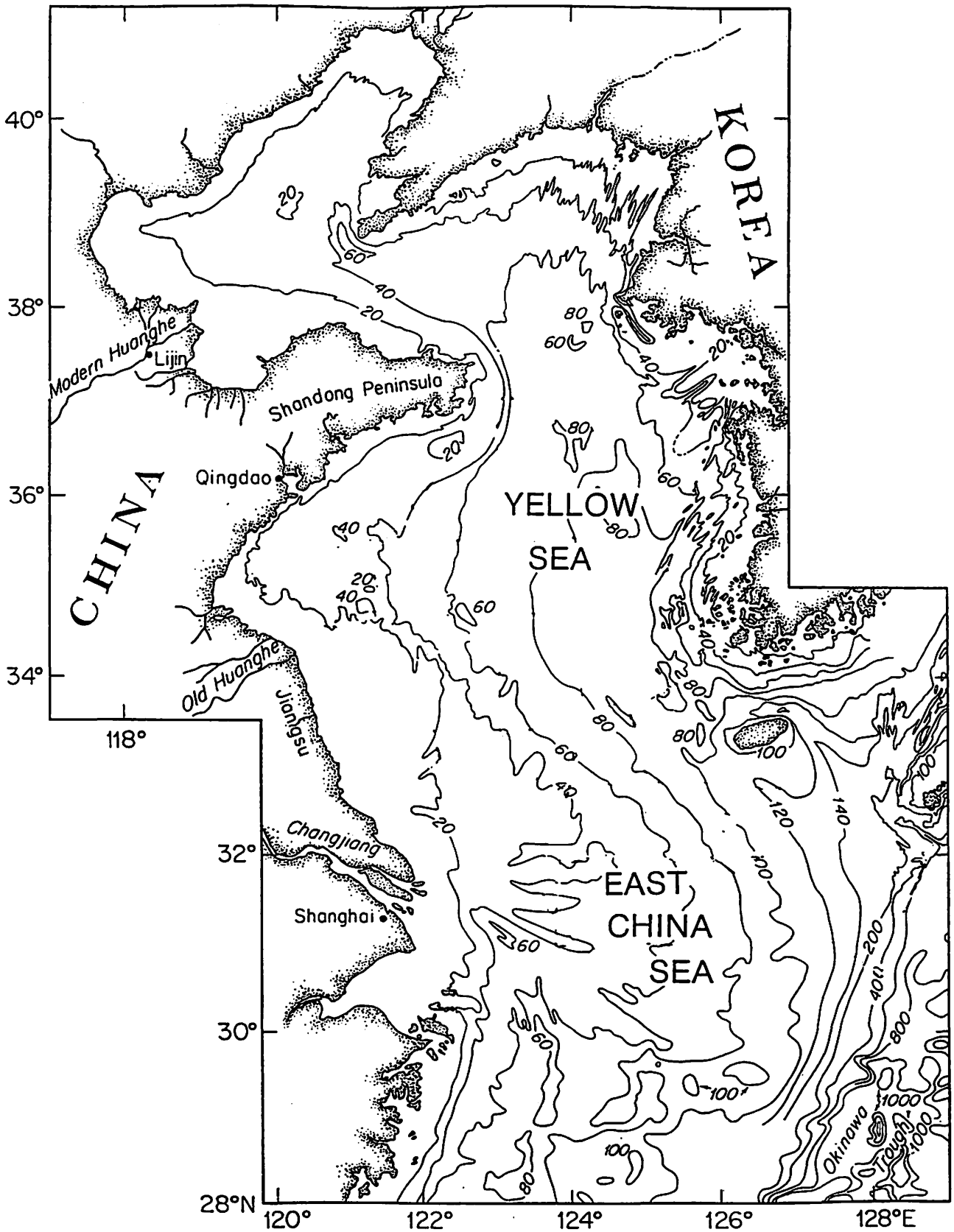

Figure 1. Bathymetric map of the Yellow and East China seas. Isobaths are in meters.

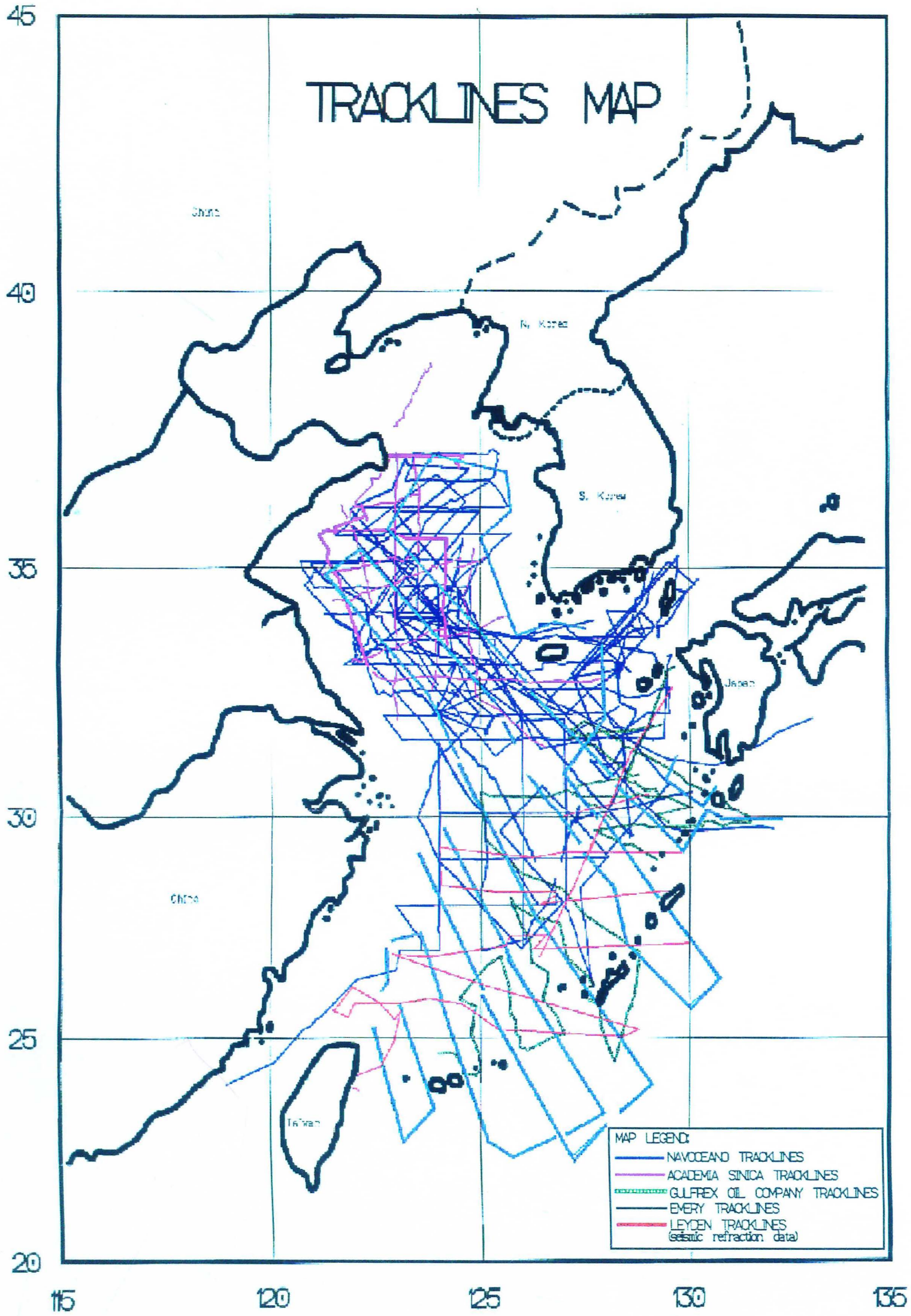

Figure 2. Location of seismic reflection and refraction profiles utilized in this study. Data come from three main sources: The U.S.-ECAFE geophysical study (Emery et al., 1969), various U.S.-Chinese cruises in the early and mid 1980's, and an extensive NAVO data base collected since the late 1980's. The locations of several available multi-channel profiles obtained by Gulf Oil are also shown.

In the 1970's the Gulf Oil Company collected a number of 48-channel, 5 second sweep seismic profiles in the southern East China Sea and adjacent Okinawa Trough. These profiles, which display the depth and nature of the acoustic basement, are analog and no velocity data are given. However, by integrating these profiles with LDGO seismic refraction data, we can get a good impression of the seismic velocities of various sediment layers. The Geological Survey of Japan collected additional data in the Okinawa Trough in the late 1970's, mostly single-channel air gun and 3.5 kHz profiles.

Finally, NAVO has collected considerable data through its on-going collection of 3.5 kHz and shallow sparker data in the YS-ECS. Unfortunately, the 3.5 kHz data appear on 1-sec sweep profiles, thereby not giving sufficient vertical resolution to allow a good delineation of Holocene sediment thickness. As a result, the Holocene isopach map given in this report generally is based on the WHOI-ACS data, all done on a 1/4 second sweep, which allows for much better vertical resolution.

Collectively, then, there is a considerable amount of geophysical data in the study area, and this can be ground-truthed to some extent with the access to geological logs of exploratory holes drilled by petroleum companies.

In addition to these geophysical data, detailed suspended matter, light transmission data, and CTD data were collected on all of the WHOI-IO/AS cooperative cruises, thus giving us picture of both the spatial and temporal distributions of these parameters throughout the entire area. There also are many peripheral data that have been collected and reported on in the scientific literature, particularly in Chinese earth science and oceanographic journals.

This Report

Discussion of the Yellow and East China seas in this report includes a literature review, much of which was covered more briefly by Milliman and others (1989). Contrary to some literature reviews, however, this report does not attempt to list every relevant (and many non-relevant) paper written on the study area, as a comprehensive annotated bibliography was submitted to NAVO in 1996 (Scott et al., 1996). The interested reader can access the primary literature through a key-word index program that accompanies that bibliography.

Most of the original research covered in this report involves the analysis and integration of seismic reflection profiles collected by the various research programs in the Yellow and East China Seas. As mentioned above, the quantity of data is large, but the types of data and their quality vary considerably.

The basic geological framework was first defined on the basis of the U.S.-Chinese geophysical data collected by the senior author in the early 1980's. These data include both high-resolution and deeper seismic data that can define the sediment cover as well as the thicker Neogene record. Into these data were merged the NAVO data. After that, other data, such as from Emery et al. (1969) were added.

Two other primary tasks have been integrating a geological picture derived from the analysis of the seismic reflection profiles with data obtained from seismic refraction profiles. This is particularly important because of the very local extent of sonobuoy data taken by Lamont-Doherty Geological Observatory (LDGO) in the late 1960's and early 70's (Fig. 2). This was done primarily by relating our structural map (e.g. Fig. 25) with the structure derived by LDGO scientists based only on seismic refraction data. Differences between the two interpretations provided the basis for a discussion on the lateral and vertical shift in facies during the early Neogene (see below).

Interestingly, by relating the seismic reflection and refraction data, we have then back-integrated such that we can speculate on the acoustic nature of the deeper reflectors in the northern East China Sea and the Yellow Sea in the complete absence of seismic refraction data.

These analyses have resulted in a series of maps, the ones of particular interest showing the thickness of Neogene sediments and an adjoining structural map. These, along with several other maps, are presented in double page-size form within the present report.

All seismic reflection data upon which these maps were based have been scanned and stored in digital format. A total of 13 CD-ROMs were collected into a single folder, along with maps showing the ship tracks for the data on each CD-ROM; The folder containing these CD-ROMs was submitted to NAVO in early 1997.

We have concluded this report with a short section on future studies in the area. Of prime importance will be detailed studies of specific areas of particular interest.

Regional Character

The Yellow and East China seas have several characteristics that set them apart from other areas in the world. First, as discussed above, these seas represent a broad, shallow epicontinental sea - there being 750 km from the Shandong Peninsula to the Okinawa Trough (Fig. 1).

Second, the Yellow and East China seas have two of the world's largest rivers discharging into them - the Huanghe (Yellow River) and the Changjiang (Yangtze River), which together have discharged more than 1.5 billion tons of sediment annually for at least the past 2500 years. Before that time, the Huanghe's load apparently was about an order of magnitude smaller, increasing only after the loess hills of northern China began to be tilled and farmed, hence accelerating land erosion (Milliman et al., 1987). Rivers draining the Korean peninsula (e.g., Yalu and Han) discharge orders of magnitude less sediment, so that the sediments off western Korea generally reflect a Huanghe mineralogy.

It is also of interest to note that the path of the Huanghe has changed markedly within recorded history as well as during pre-historical times. Prior to 1128 AD, for instance, the river discharged into the Bohai (Fig. 3). It then bifurcated, part of the river discharging to Jiangsu coast south of the Shandong Peninsula. Beginning in 1495, the river discharged exclusively to the Jiangsu coast, but then changed its course again in 1855 to the Bohai. The sedimentary regime of the South Yellow Sea, however, still reflects the old path of the Huanghe, even though it has flowed north for more than 100 years.

Third, the Yellow and East China seas have a huge demographic pressure on them, as reflected by the nearly one billion people who live within the watersheds of the rivers that drain into these seas. The combination of large populations and the influence of large rivers (as well as regional oceanography - see below) means that the Yellow and East China seas are heavily fished, fishing trawl marks often representing the major morphologic feature in the South Yellow Sea.

Finally, although it will be discussed in greater detail below, mention should be made of the regional land geology, much of which is also noted in the deeper submarine geologic structure. Two structural highs extend SW-NE across China to the Korean peninsula - The Shangdong-Laoyehling Massif in the north, and the Fukien-Reinan Massif in the south (Figure 4). In addition, the Taiwan-Sinzi Folded Zone along the outer edge of the East China Sea indicates the subduction from the Okinawa Trough backarc basin. The backarc basin - oceanic boundary is marked by the Ryuku Folded Zone on which a number of uplifted islands are present, the most prominent being the island of Okinawa.

Bathymetry, Surficial Sediments, and Seafloor Morphology

The Yellow and East China seas are characterized by a broad, shallow epicontinental shelf, generally less than 100 m in water depth. The northern Yellow Sea, located between the Gulf of Bohai and the northeastern tip of the

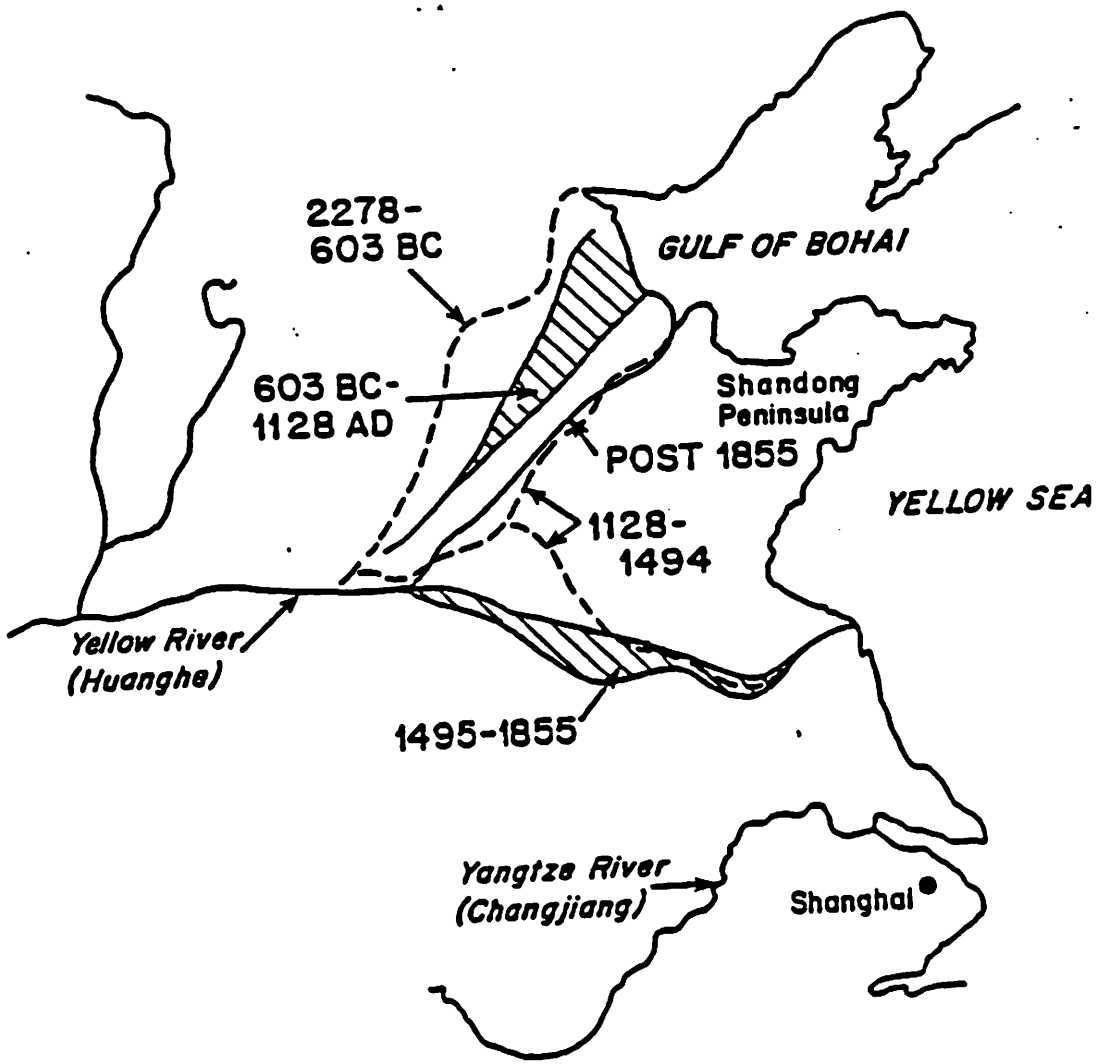

Figure 3. Discharge paths of the Huanghe during the past 4000 years.

Shandong Peninsula, is mostly less than 60 m in depth. The southern Yellow Sea, south of the Shandong Peninsula and 32° N latitude, is mostly less than 100 m deep, the western part of the area is mostly less than 60 to 80 m in depth (Fig. 2). The East China Sea, south of 32° N latitude, is characterized by a broad prograding delta off the Changjiang, with water depths mostly less than 60 m. To the east, south of Cheju Island, water depths increase to greater than 140 m. The Okinawa Trough lies to the south of the East China Sea, with depths increasing markedly at the 120 to 140 m isobaths. Maximum water depths in the Okinawa Trough exceed 1000 m.

Many authors have written on the character of Yellow and East China sea sediments (e.g., Nino and Emery; Wang, 1982; Qin and Li, 1983; Jeong et al., 1984). Because each of these authors used slightly different sediment classifications, the sediment distribution has been simplified somewhat for this report. In general the sediments can be characterized as a multi-layered sandwich, with coastal sediments along both the Chinese and western Korean coasts being dominated by silty and clayey muds, as is much of the central portion of the study area (Fig. 5). Situated between the central and coastal muds are two zones of sandy sediments, which as will be seen in a following section, represent relict sediments deposited during the last low stand of sea level and its subsequent transgression The muds, in contrast, are assumed to be modern (see below).

Numerous side-scan sonar profiles obtained by the senior author indicate that the muddy coastal and central sediments are generally featureless, the major feature being fishing trawl scars. Much of the southern Yellow Sea dominated by muddy sediments, in fact, is so featureless that topographic relief is seldom more than a fraction of a meter; one seismic line run south of the Shandong Peninsula, in fact, covered more than 200 km with no more than 2-4 m of total relief - far less relief than one sees in most abyssal plains. No evidence of recent slumps has been noted in the Yellow or East China Sea, although such slumps are common in the Okinawa Trough. At least one location off the Changjiang delta displays show pock marks related to the escape of biogenic methane gas (Fig. 6); undoubtedly more detail of this area would show a greater distribution of pock marks.

In contrast, the sandy areas in the East China Sea have sand waves and ridges, often capped by a rippled bottom up to 1 m in amplitude (Fig. 7). Much of the inner shelf off western Korea is dotted with what appear to be sand ridges up to 10 m in relief). High-resolution seismic profiles show that at least some of these ridges are capped with up to 5 m of acoustically transparent sediment, which we assume to be modern in age (Fig. 8). Although the morphology, shallow structure and age of these sand ridges are not known, they together with the rippled seafloor seen elsewhere in the East China provide evidence of the local mobility of seafloor sediments.

Regional Oceanography

Circulation in the study area is dominated by the northward flow of two loops of the Kuroshio Current, the Taiwan Warm Water (TWW) in the

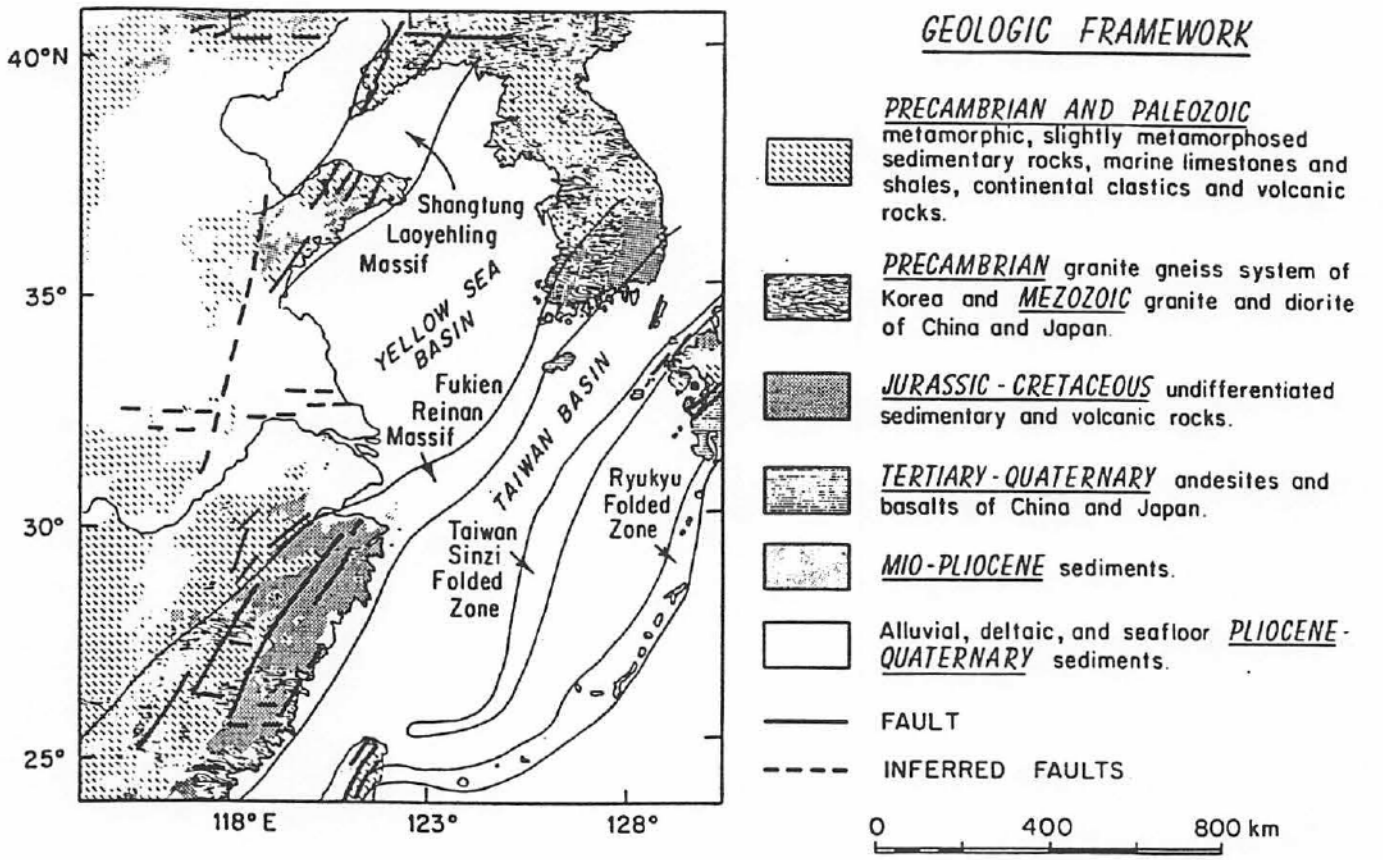

Figure 4. General geology of eastern China and Korea, showing the structural highs (massifs) that dominate deep structure of the Yellow and East China seas. After Emery et al. (1969).

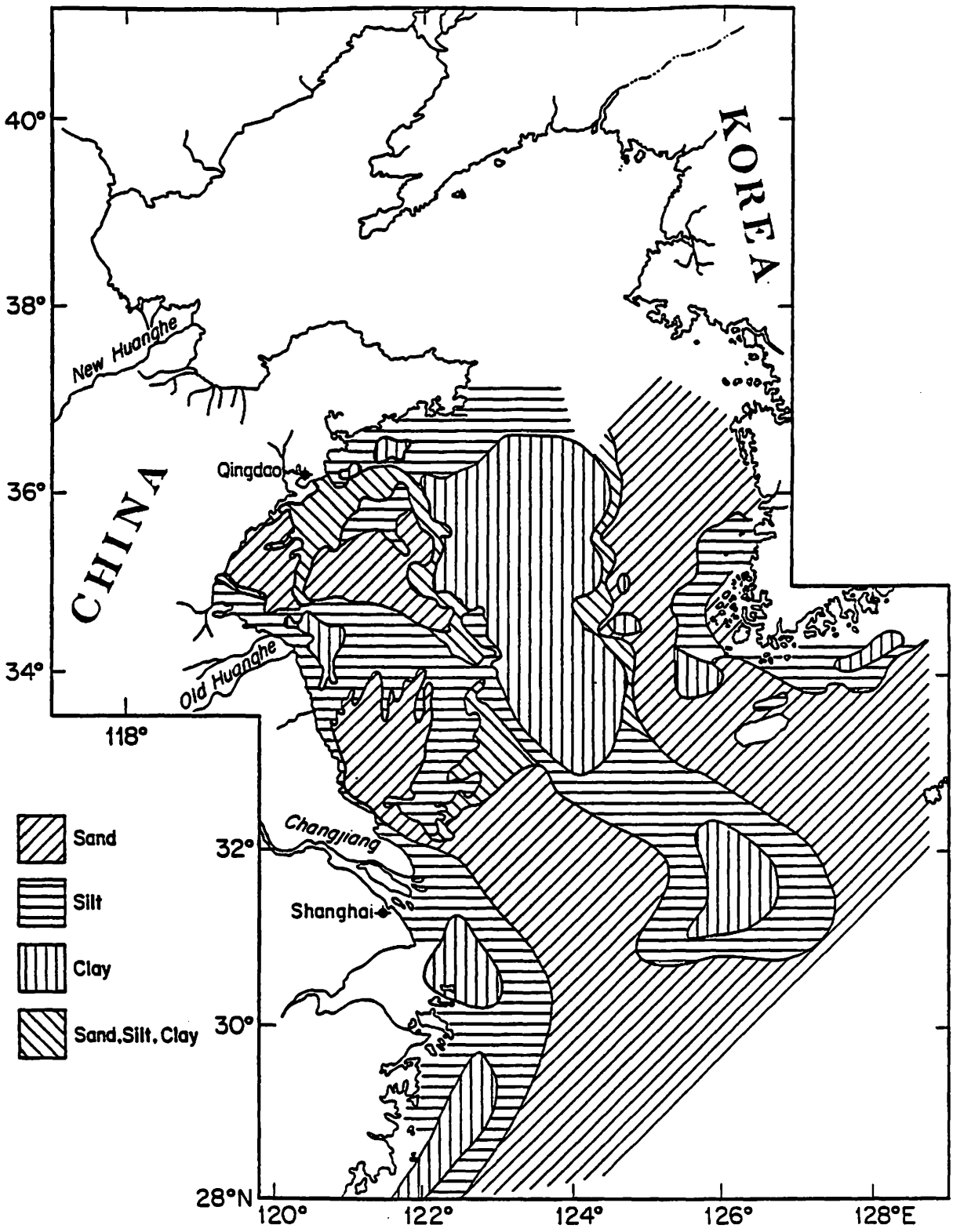

Figure 5. Surficial sediments of the Yellow and East China seas. After Wang (1982), Qin and Li (1983) and Jeong et al. (1984).

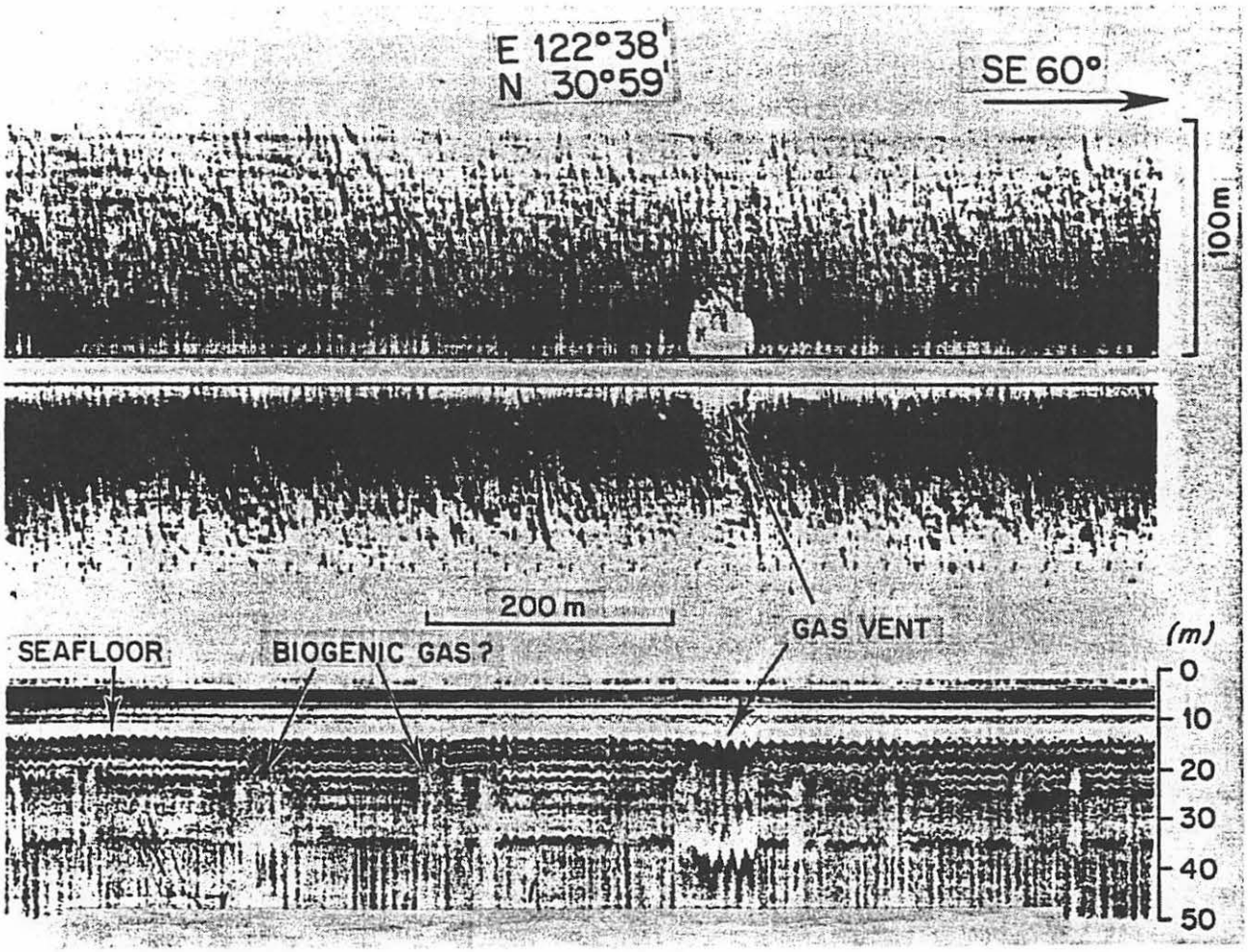

Figure 6. Side-scan sonar profile (upper) and 3.5 kHz profile (lower) of an area in the inner shelf off the Changjiang showing a methane gas vent. Other than this single gas vent, the seafloor in this area is featureless, the noise in this record a function of the rough sea state. After Butenko et al. (1985)

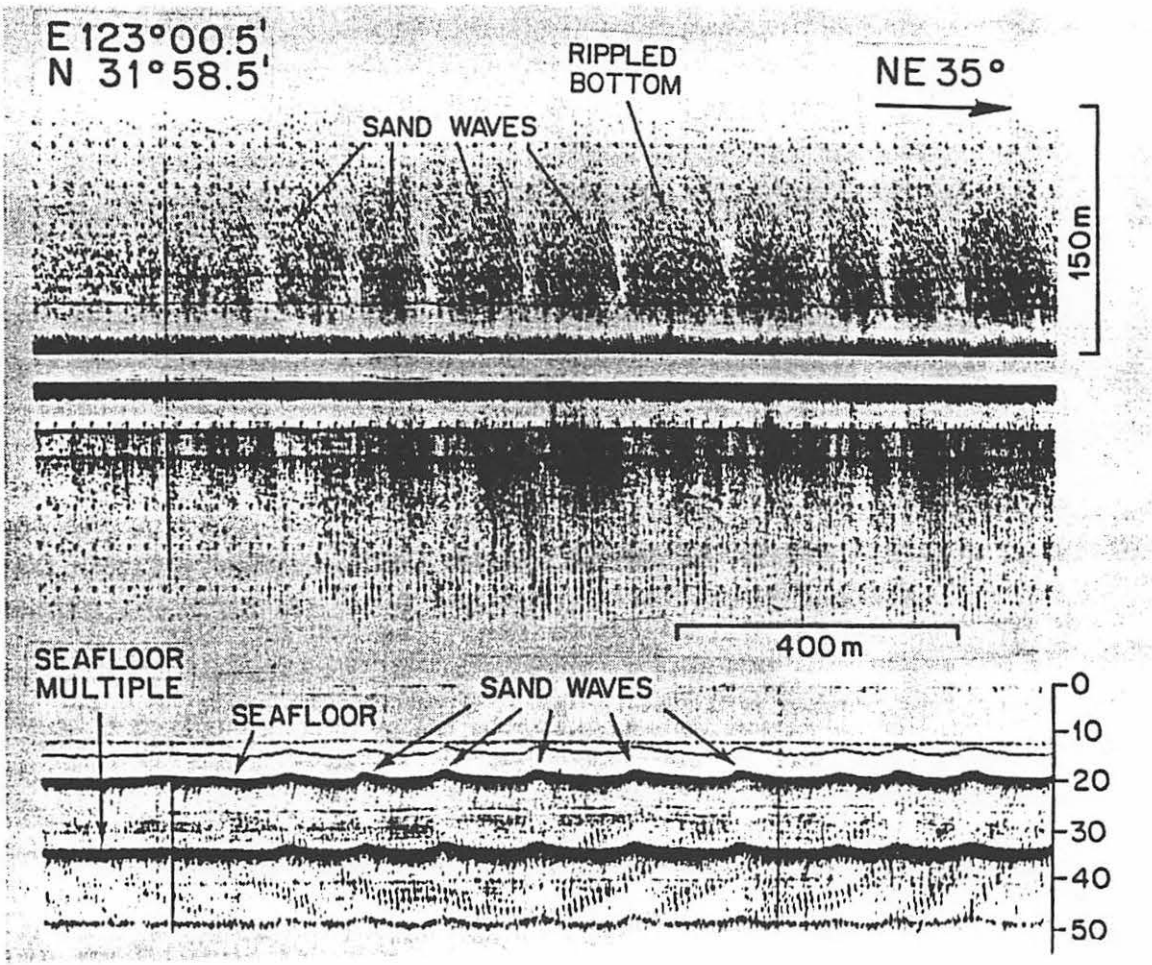

Figure 7. Side-scan sonar profile (upper) and 3.5 kHz profile (lower) of a sand-wave field on the mid shelf off the Changjiang mouth. Note that sand ripples are superimposed on the sand waves. Subbottom strata seen in the 3.5 kHz profile are sub-horizontal. After Butenko et al. (1985).

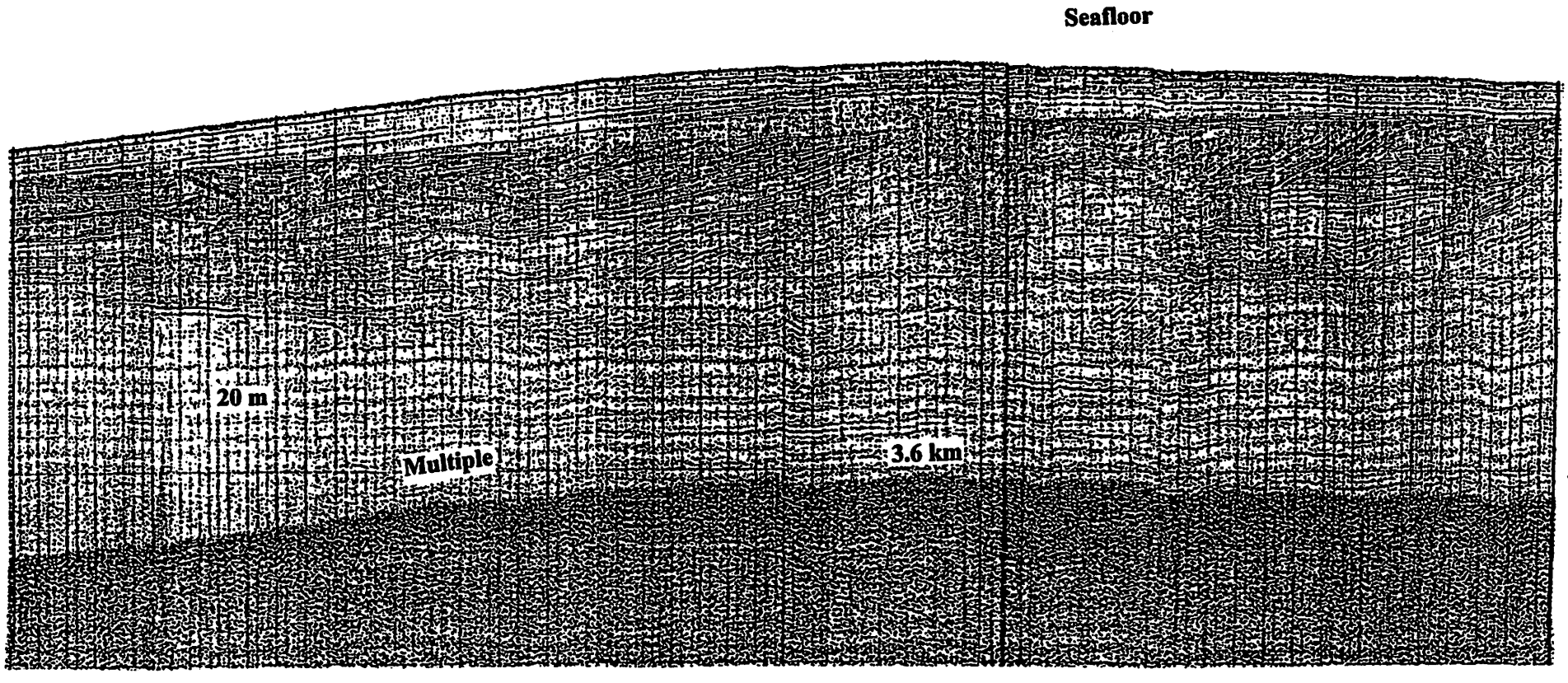

Figure 8. Huntec DTS profile of a sand wave north of Cheju Island. Note that the fine-grained sand is acoustically transparent and is up to 5 m thick on top of the sand wave, but less than 1 m thick on the sides.

west and the Yellow Sea Warm Water (YSWW) in the east. Both water masses are characterized by high salinities and warm temperatures. In contrast, southward flow in nearbottom waters occurs by flow of the Changjiang and Jiangsu coastal waters (CJCW and JCW, respectively) along the Chinese, the Korean Coastal Water (KCW) in the east, the Yellow Sea Cold Water (YSCW) in the north (Figure 9). These coastal currents appear as seasonally cold and brackish water masses related to cold outbreaks in the winter (compare Figs. 10, 11).

One result of this regional circulation pattern is its effect on the suspended matter concentrations in various water masses. Being oceanic in origin, the TWW and YSWW tend to have low suspended mater concentrations, generally less than 1 mg/l; interestingly, these water masses overlie the sandy sediments on either side of the central mud patch (compare Fig. 5 with Figs. 10 and 11).

Superimposed on this regional picture, however, is a strong seasonal imprint. In summer, winds come from the south and tend to be gentle (except, of course, for typhoons). Combined with the dominant outflow from the Changjiang, the summertime water column tends to be stratified, and therefore resuspended sediment tends to remain confined to the very nearbottom waters below the pycnocline; only locally do nearbottom concentrations reach 10 mg/l, and surface concentrations often are less than 1-2 mg/l (Figs. 10, 12).

In contrast, wintertime circulation is dominated by arctic air outbreaks from the northwest. The water column tends to be well-mixed, temperatures and salinities increasing towards the YSWW in the east (Figs. 11, 13). Associated wind-driven currents enhance southeastern flow of the JCW, and as a result, a turbid plume of nearbottom water extends from Jiangsu southeast to as far as Cheju Island. Wintertime nearbottom suspended matter concentrations locally can exceed 80 ppm in coastal waters, and concentrations greater than 10 mg/l can extend far to the south, often associated with the central mud patch (compare Figs. 5, 11 and 12). Moreover, in shallow waters, even surface concentrations can exceed 20 mg/l.

Modern Sediment Sources

Based on mineralogy, basically the presence or absence of terrigenous calcite, Milliman et al. (1985) were able to show that the western South Yellow Sea and the mid-shelf mud patch are derived mainly from the Huanghe, whereas the western East China Sea sediments are mostly Changjiang-derived. This agrees closely with the oceanographic observations cited above, which indicate a southward transport of Huanghe sediments from the Jiangsu coast during winter storms. Changjiang sediments, on the other hand are deposited off the Changjiang estuary during peak summer flow and then resuspended and transported directly southward during winter storms (DeMaster et al., 1985). Apparently very little of this sediment escapes to the mid-shelf mud patch, as suggested by the clear TWW.

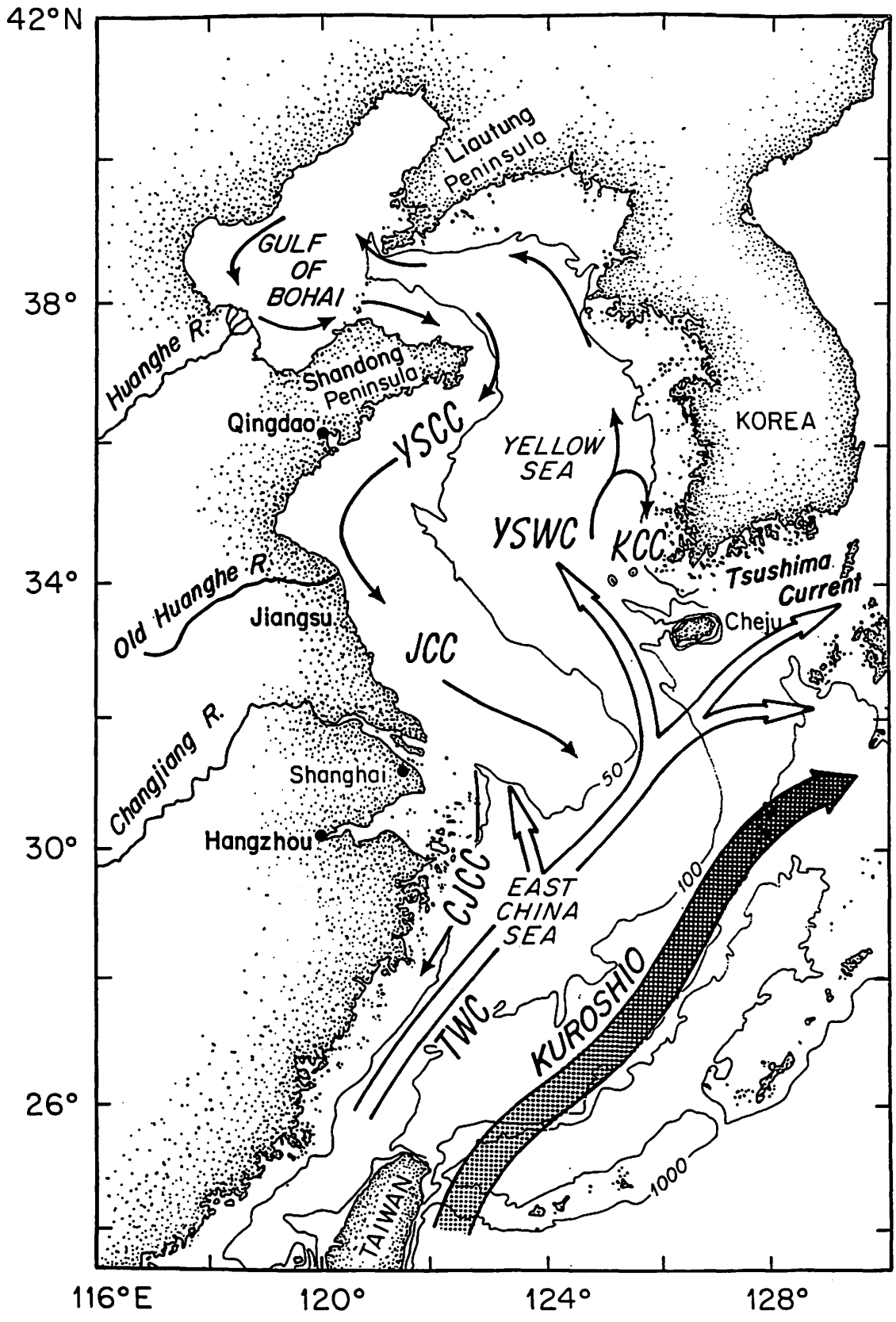

Figure 9. General circulation patterns in the Yellow Sea and East China Sea.

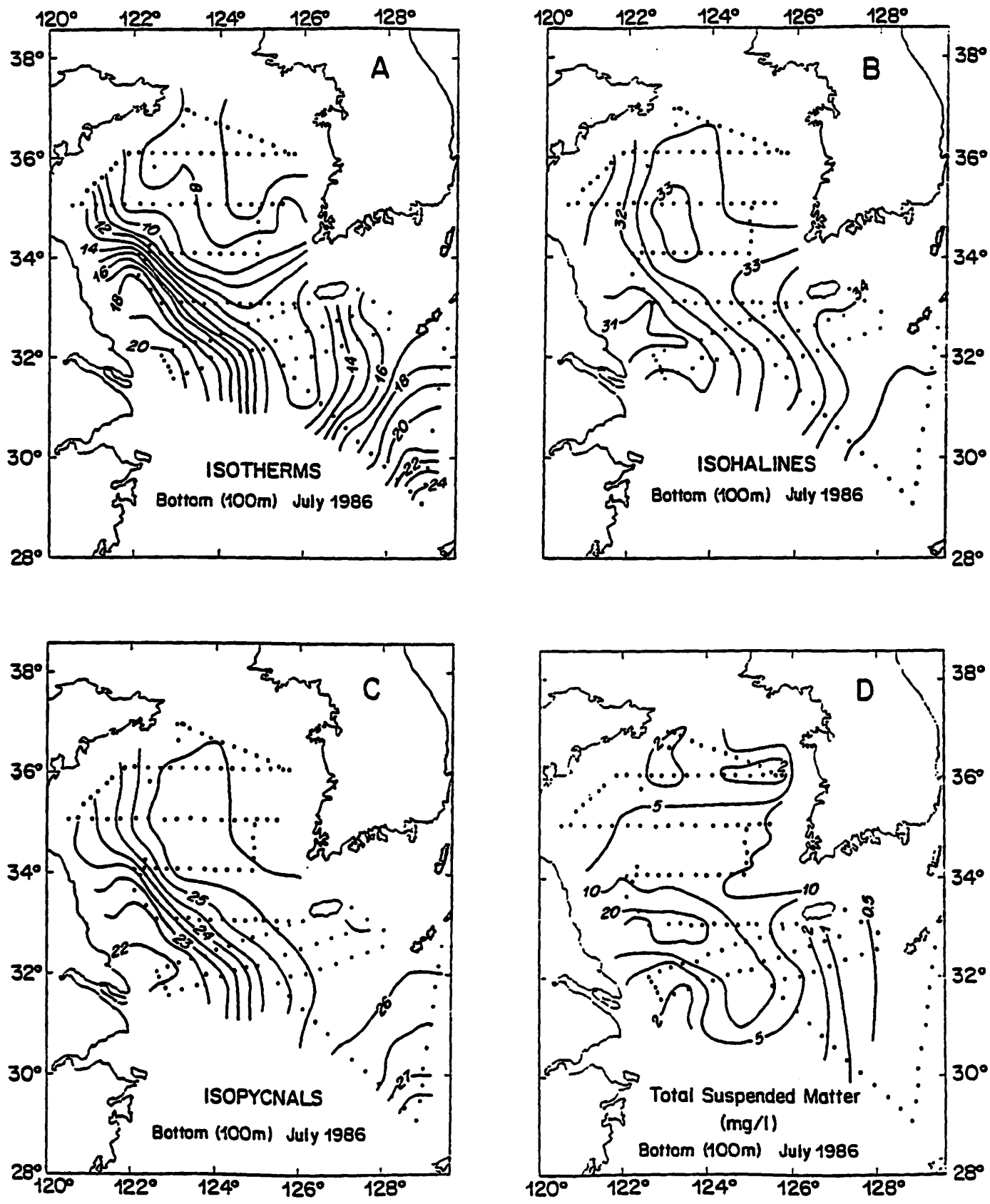

Figure 10. Distribution of water temperature, salinity, water density and total suspended matter in nearbottom waters in July 1986. From Milliman et al. (1989).

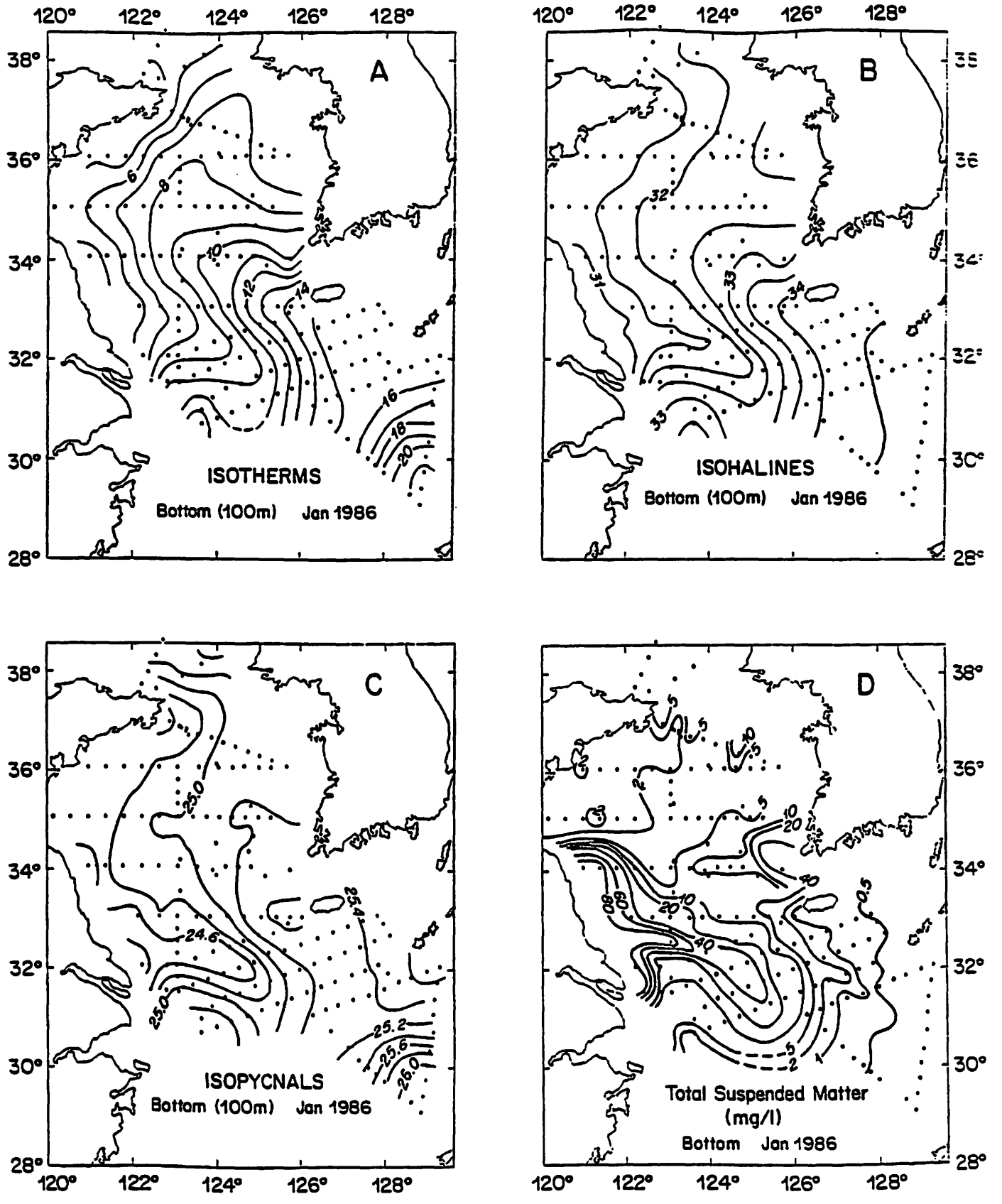

Figure 11. Distribution of water temperature, salinity, water density and total suspended matter in nearbottom waters in January 1986. From Milliman et al. (1989).

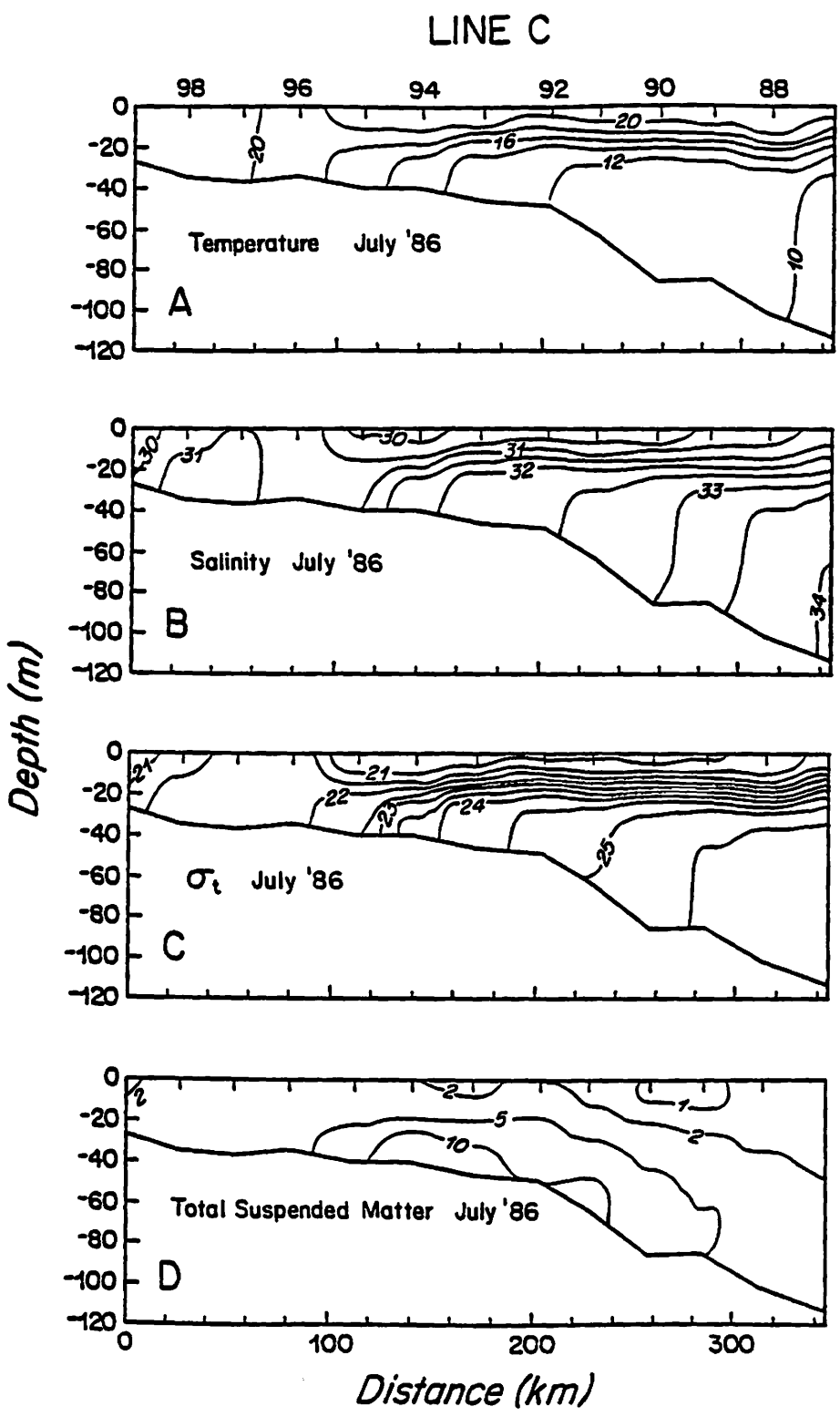

Figure 12. W-E profile of watertemperature, salinity, water density and total suspended matter across the southern Yellow Sea between the north shore of the Changjiang and the west coast of Cheju Island in July 1986. Note the well stratified nature of the waters and the relatively low concentrations of suspended matter, even in the bottom waters. From Milliman et al. (1989).

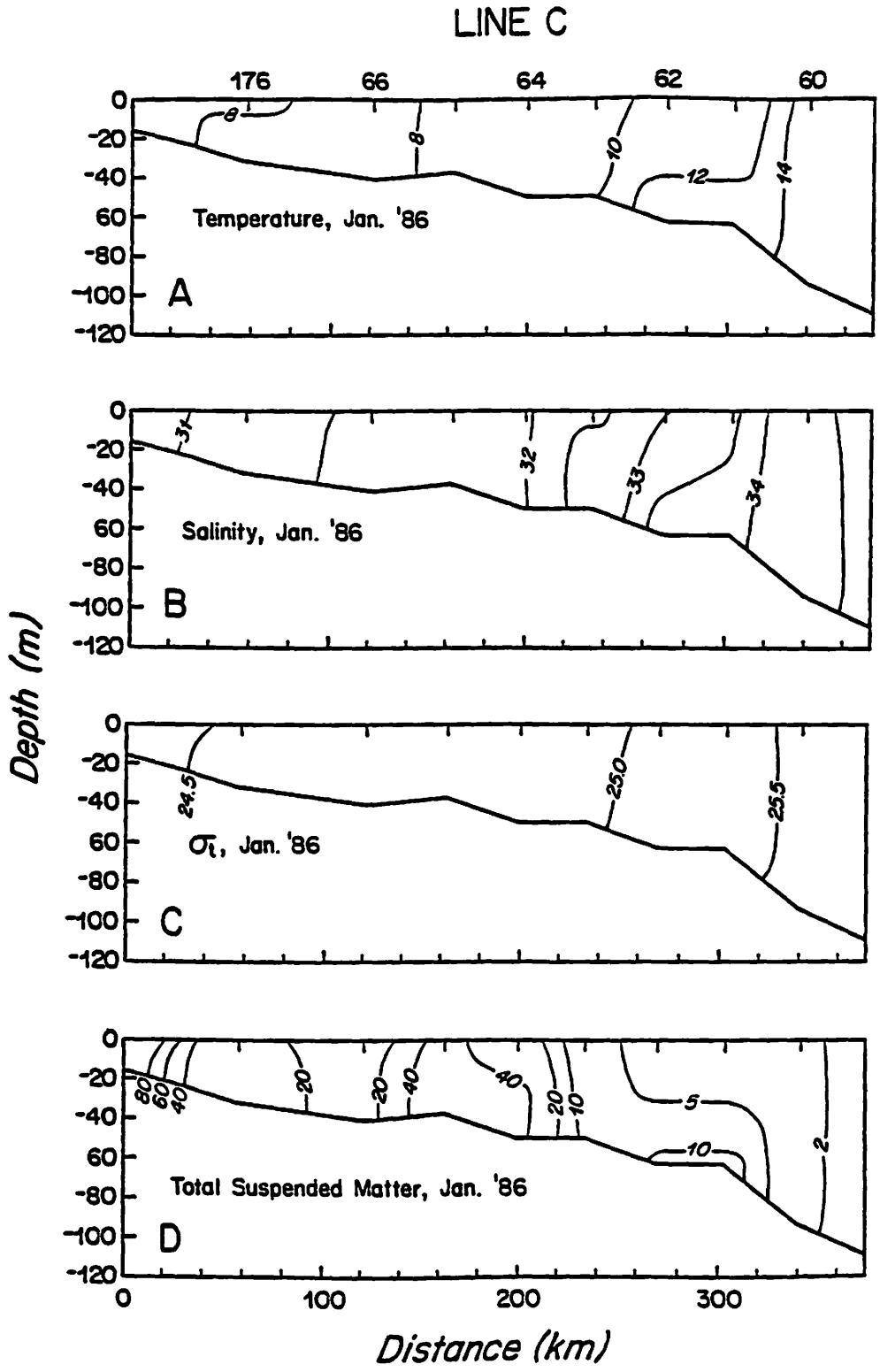

Figure 13. W-E profile of watertemperature, salinity, water density and total suspended matter across the southern Yellow Sea between the north shore of the Changjiang and the west coast of Cheju Island in January 1986. Note that the water column is well mixed and locally suspended matter exceeds 40-80 mg/l. From Milliman et al. (1989).

Geotechnical Character of Surface Sediments

Very few studies have been published on the geotechnical character of seafloor sediments in the Yellow and East China seas. To the present writers' knowledge, the best studies are those by Keller and Ye (1985) and Butenko et al. (1985) off the Changjiang. Butenko et al. (1985) listed six sediment types and average textural compositions, water contents, bulk densities, and (where applicable) shear strengths (Table 1). They showed, for instance, that the Yellow River-derived muds have much higher average water content (118 %) than Changjiang-derived silty clays (78 %), with correspondingly lower shear strengths (Table 1). Water contents of all cohesive sediments, in fact, are distinctly higher than liquid limits (Keller and Ye, 1985); this difference is particularly great on the mid-shelf mud patch, which led Keller and Ye (1985) to speculate that these deposits could fluidize upon disturbance.

Keller and Ye (1985) also noted that shear strength of cohesive sediments increased significantly in the five cores they analyzed, increasing from 2 to 6 kPa at the core surface to 5 to 10 kPa at 2 to 2.8 m core depth. These authors speculated that the increased shear strength reflected the effect of overburden. A gray clay found in Keller and Ye's Core 25 was particularly stiff and had low water content, leading those authors to conclude that the clay was relict.

Given the lack of other data, one can speculate that the modern Holocene muds probably have relatively low shear strengths (2-6 kPa), the lower values perhaps related to Huanghe-derived muds, which generally contain more silt and less (more cohesive) clay that do Changjiang-derived muds. Based on clay mineralogy studies in the area, this would mean that the coastal muds south of the Changjiang (Changjiang-derived) probably have somewhat greater shear strengths than do muds in the central portion of the East China Sea, which are Huanghe-derived. Inner shelf muds off the Jiangsu coast north of the Changjiang, although also Huanghe-derived, may have somewhat higher shear strengths than those in the central East China Sea, as these muds have been actively winnowed for the past century, since the Huanghe changed its course in 1855. Shear strength probably shows less increase with sediment depth in those areas with high Holocene accumulation rates than in sediments from areas with lower rates of accumulation.

Sediment type	Average grain size (%)				Average water content (%)	Average total unit weight ($g\ cm^{-3}$)	Average undrained shear strength (Torvane) ($g\ cm^{-2}$)
	Grav.	Sand	Silt	Clay			
Changjiang-derived silty clay (average values of sea-floor samples)	0	6	49	45	78	1.58	30
Yellow Sea-derived silty clay (average values of sea-floor samples)	0	8	41	51	118	1.41	10
Soil mixture of silt, clay and fine sand (average values of seafloor samples)	0	35	31	34	63	1.69	—
Silty fine sand (average values of seafloor samples)	1	70	14	15	—	—	—
Silty and clayey fine sand (average value of seafloor samples	0	67	20	13	38	1.84	—
Well-sorted fine sand (average value of sea-floor samples)	2	92	6	6			

Table 1. Geotechnical properties of various sediment types in the western and central East China Sea off the Changjiang. After Butenko et al. (1985).

Late Quaternary/Holocene Seismic and Sedimentologic Record

The late Quaternary history of the Yellow and East China seas has been dominated by fluctuating sea levels related to glacial and interglacial cycles. During the last glacial epoch, for example, sea-level in the East China Sea was about 120 m lower than at present (Emery et al., 1971), meaning that at that time the Chinese rivers discharged almost directly into the Okinawa Trough.

Evidence of fluctuating sea level is seen high-resolution seismic ORE Geopulse and 3.5 kHz data, together with EG&G Uniboomer and Huntec DTS profilers, reveal a series of repetitive cycles in the shallow seismic (Quaternary) record. The lower boundary of the most recent cycle is characterized by a prominent erosional surface, often 10 to 50 m beneath the seafloor (Fig. 14). Locally this erosional surface is cut by channels that in the western part of the South Yellow Sea appear to be oriented along E-W drainage patterns that merge east of 124° E with broad meandering N-S channel system in water depths greater than 80 m. Southeast of Cheju Island, the channel system is seen as several buried channels (Fig. 15).

We assume that this erosion surface formed during the last regression of sea level, 70 to 80 thousand years ago, and that the meandering channels are relics of the meandering Huanghe during the subsequent low-stand of sea level. Overlying the erosion surface are horizons that we consider to be channel , and in some profiles (e.g. Fig. 14B) we can identify what appear to be point-bar deposits, suggestive of a river facies deposited during the last low stand of sea level. Landward, this river-channel facies grades into a deltaic facies (Fig. 15), formed when the Huanghe flowed south of the Shandong Peninsula during a subsequent higher stand of sea level, perhaps during a slight warming period 25-35 thousand years ago. A prominent erosional surface within this delta also can be seen (Fig. 15).

Overlying this sedimentary sequence is an acoustically dark layer, overlain by an acoustically clear layer, which can be seen in Fig. 14B). Where the acoustically dark layer has been cored, a marine peat is often noted. Several C-14 dates of this peat layer indicate that it is 9 to 12 thousand years old (Xu et al., 1982; Yang et al., 1985), suggesting that it was deposited during Holocene transgression of sea level. In the outer East China Sea, however, the transgressive sequence is thin or absent, as are modern sediments; as a result, surface sediments are sandy and often contain relics of former low stands of sea level, such as intertidal oyster shells (e.g., Emery et al., 1971; Wang and Wang, 1982; Yanagida and Kaizuka, 1982; Chen et al., 1985; Han and Meng, 1987).

The acoustically transparent layer is assumed to represent the high-stand sedimentary sequence. These deposits are thickest (up to 30 m) off the Changjiang and Huanghe, and a wedge of sediment just east of the Shandong Peninsula (Fig. 14) exceeds 40 m in thickness (Fig. 15). We are not sure if this Shandong mud wedge is entirely modern, parts of it are modern or if it was deposited entirely during the Holocene transgression.

Two zones with little or no Holocene sediment cover coincide with the sandy sediments seen in Fig. 5. In addition, a small zone just south of

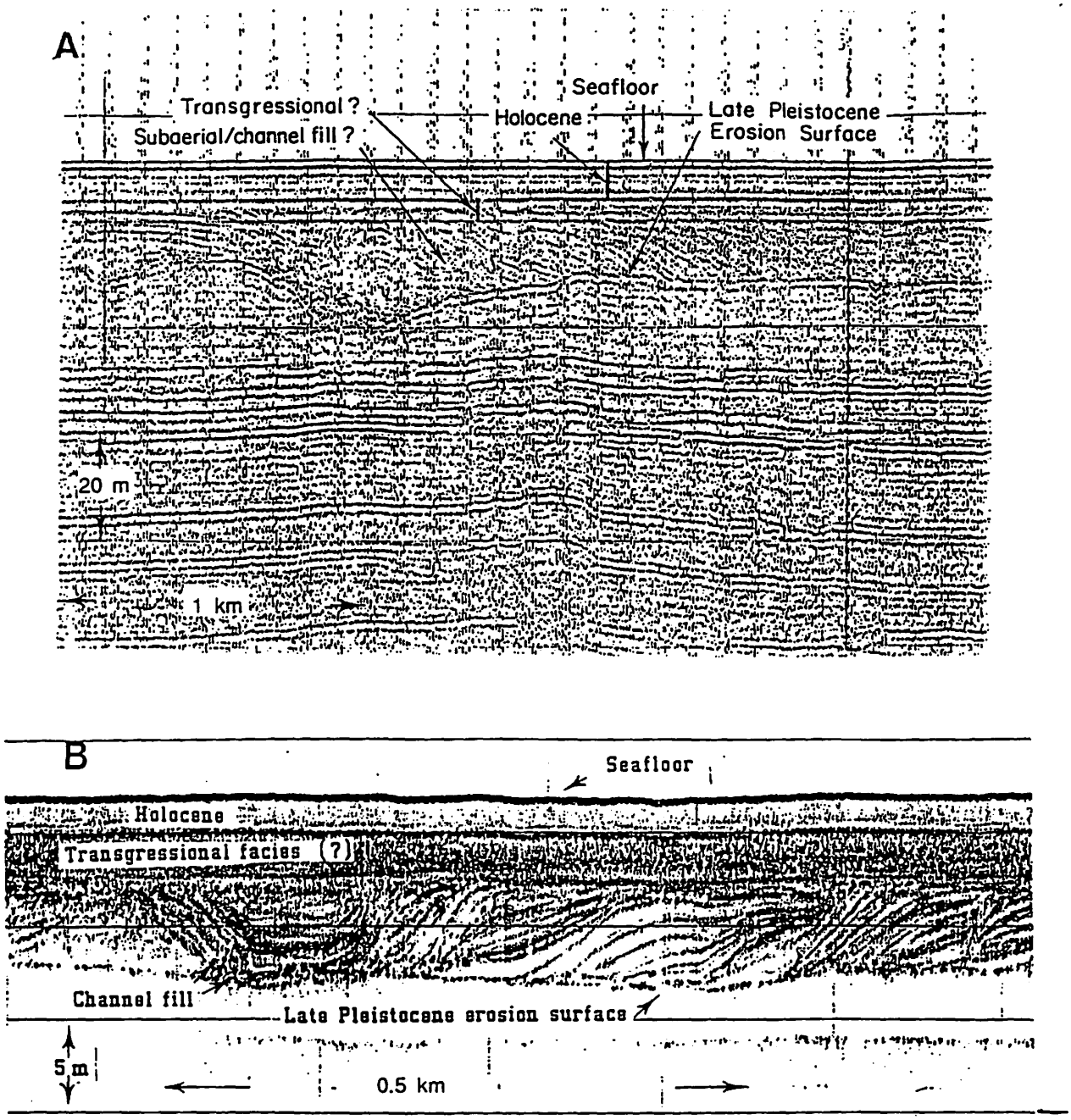

Figure 14. High-resolution seismic profiles from the South Yellow Sea showing the regressional erosion surface, subaerial channel fill, late Pleistocene-early Holocene transgressive facies, and Holocene neritic sediments. A) is an ORE Geopulse profile; B) is an ORE 3.5 kHz profile. From Milliman et al. (1989).

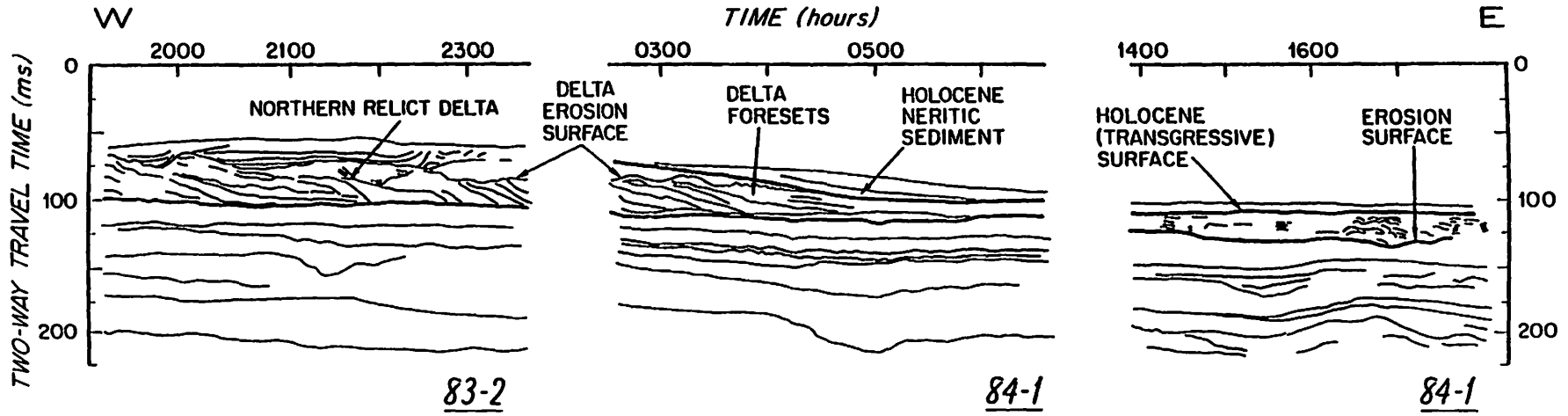

Figure 15. Interpreted W-E Geopulse seismic profile across the South Yellow Sea, showing an exposed relict delta in the west. The erosional surface is associated with the last major regression of sea level, and is seen in seismic profiles shown in Fig. 11. From Milliman et al. (1989).

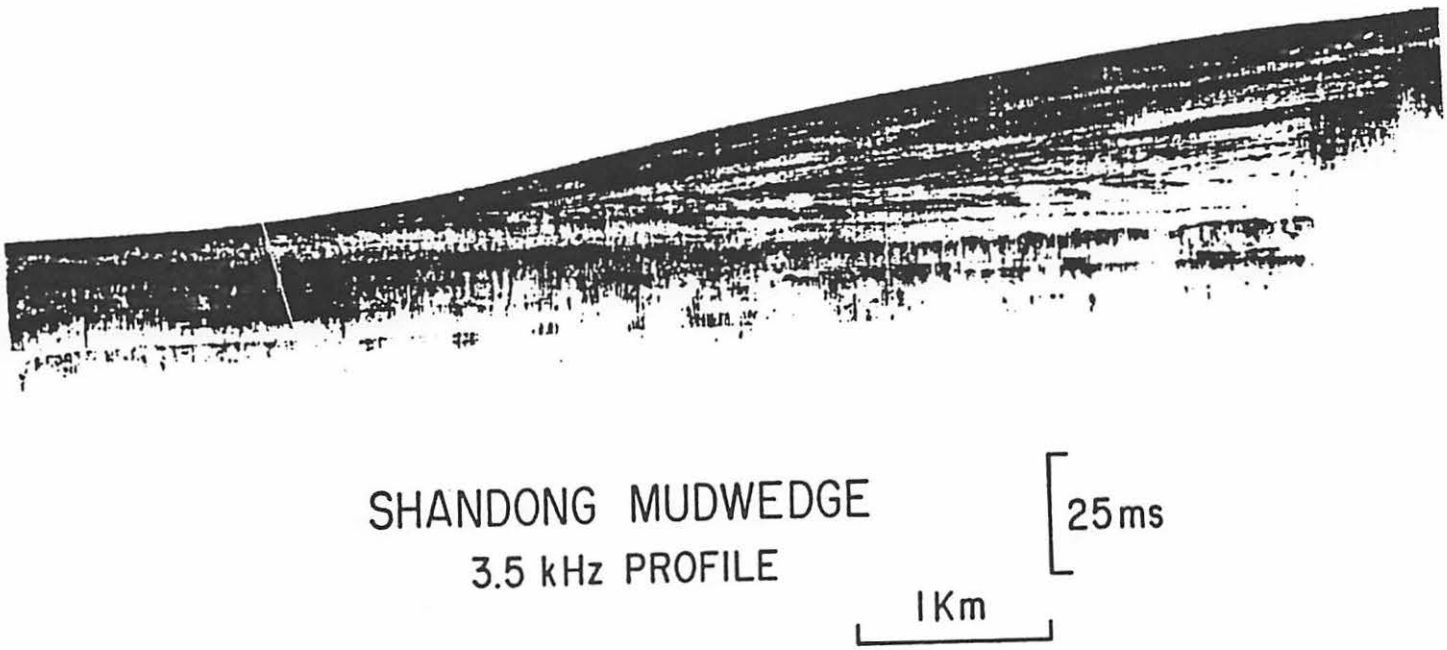

Figure 16. N-S 3.5kHz profile across the Shandong mud wedge. The prominent reflector underlying the entire sequence is thought to represent the regressional erosion surface, although the actual age of the mud wedge is not known. From Milliman et al. (1989).

Qingdao in the western South Yellow Sea (Fig. 17) has relict deltaic sediments that are exposed at the seafloor. The correlation between Holocene sediment thickness and surface sediment texture, however, is not as simple as one might imagine. Sandy sediments do not necessarily infer relict sediment, and muds do not necessarily represent rapid accumulation. For instance, the sands in the western South Yellow Sea are relict, but the sands off Jiangsu are deltaic sands deposited (and subsequently winnowed) within the past 500 years. The texture and thickness of seafloor sediment therefore reflect both recent sedimentary history and the modern oceanographic climate.

Buried Gas

Shallow, buried gas can be recognized in seismic records in several ways, the most common being a blanking out of some or all reflectors, whereas deeper gas often is recognized by a change in phase in the reflector. Unfortunately, a blanking out of reflectors on 3.5 kHz records also can indicate a change in sediment facies, for example as shift from a layer fine-grained sediment to a sandier sediment (Fig.).

Because we had relatively few Uniboom, Geopulse or Huntec DTS data, we first plotted changes in reflector intensity based on our 3.5 kHz data, which showed a number of areas in which such changes were present. Several types of possible indicators were noted, from abrupt changes in the echo character to more subtle types. As can be seen in Fig. , these locations were relatively sparsely distributed.

We then used the Uniboom, Geopulse and Huntec data to see which area(s) designated by the 3.5 kHz actually results from buried gas and which probably is indicative of facies change. In fact, the only areas in which shallow buried gas is seen is in the Shandong mud wedge south of Shandong Peninsula and very locally off the Changjiang mouth (Fig.). As mentioned previously in this paper, one side-scan sonar profile off the Changjiang showed several gas vents on the seafloor and an accompanying 3.5 kHz profile showed darkened sub-bottom strata through which the gas had escaped.

It therefore can be concluded that buried gas is not common in the Yellow or East China seas, although far more data will be needed, particularly to determine the distribution of gas in those areas in which some has been delineated. We assume that infrequent distribution of buried gas reflects more relatively low biologicalproductivity, perhaps a result of the turbid waters, rather than low rates of sediment accumulation, as locally rates can exceed several cm/yr (DeMaster et al., 1985).

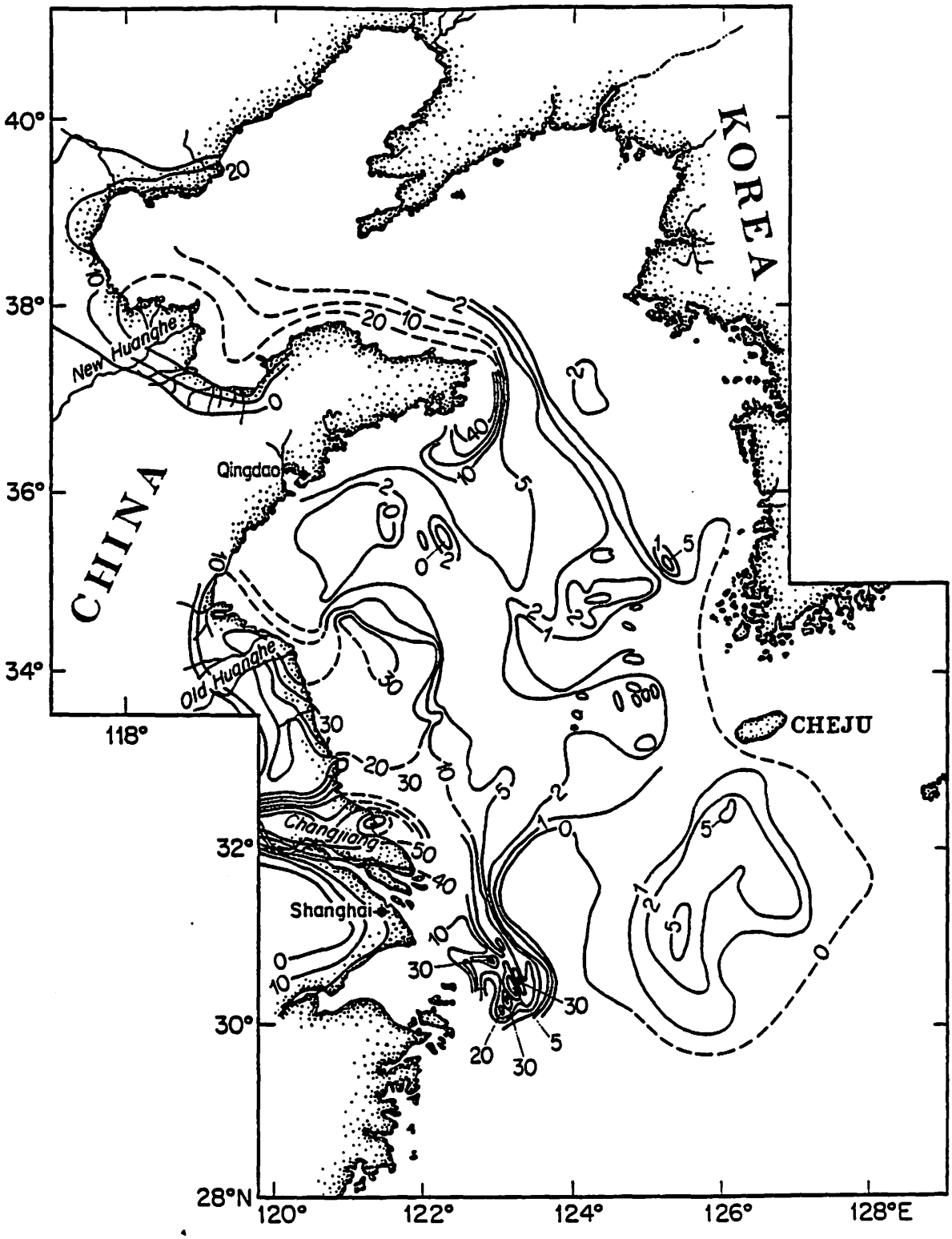

Figure 17. Thickness of Holocene sediments (in meters) in the Yellow and East China seas. The lack of data off North Korea and south of the Changjiang prevents us from delineating isopachs in those areas.

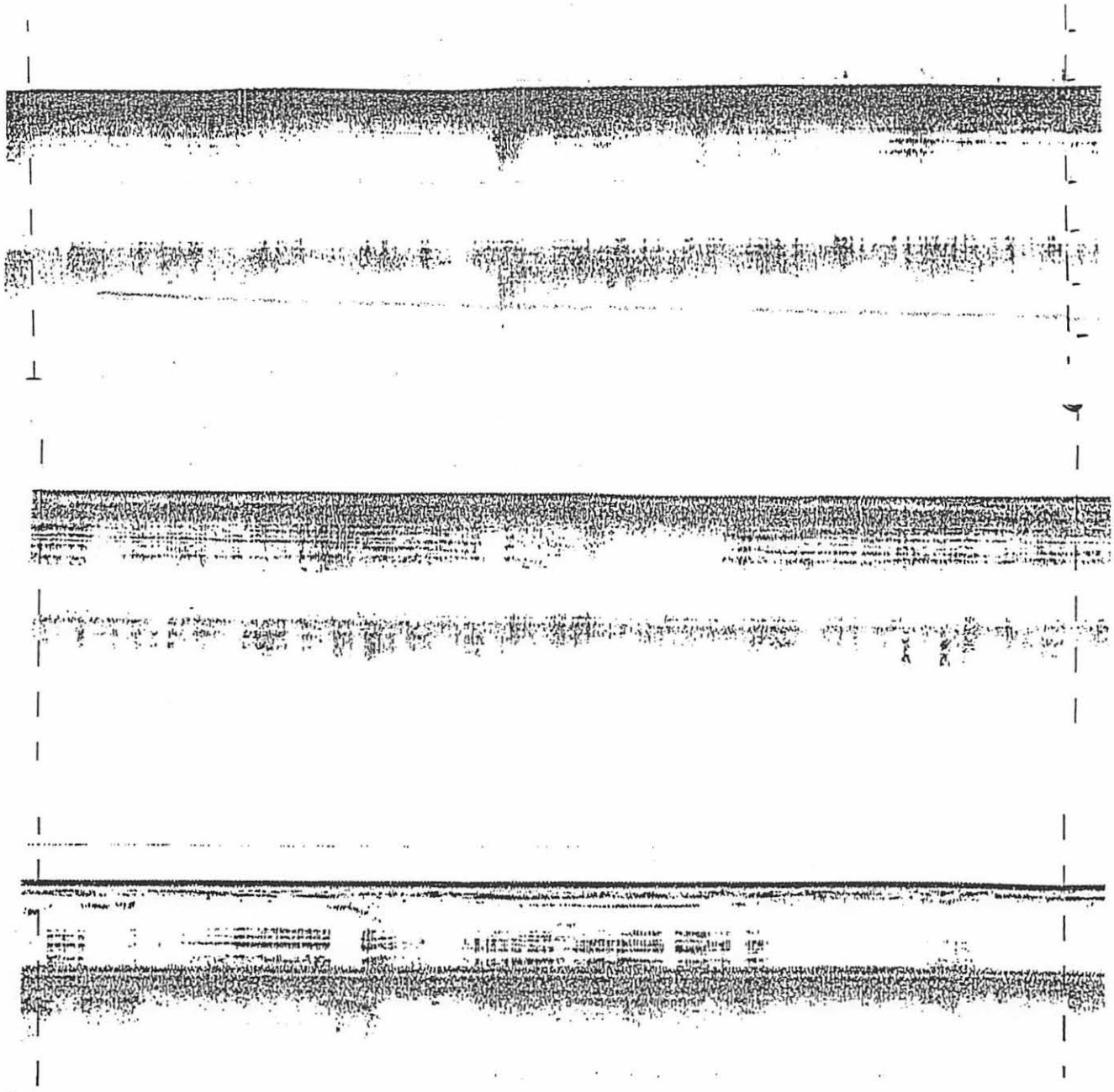

Figure 18. Examples of subtle changes in subbottom reflectors seen in NAVO 3.5 kHz records, suggestive of shallow buried gas. In Type I (upper) the surficial layer is dark and subbottoms are infrequent. In Type II (middle) the subbottom is intermittent. In Type III (bottom) acoustic penetration is deep, the record having large areas in which the reflectors are completely blanked out. Subsequent inspection of high-resolution seismic records, however, indicates that these acoustic types are probably indicative of subtle changes in facies, not buried gas.

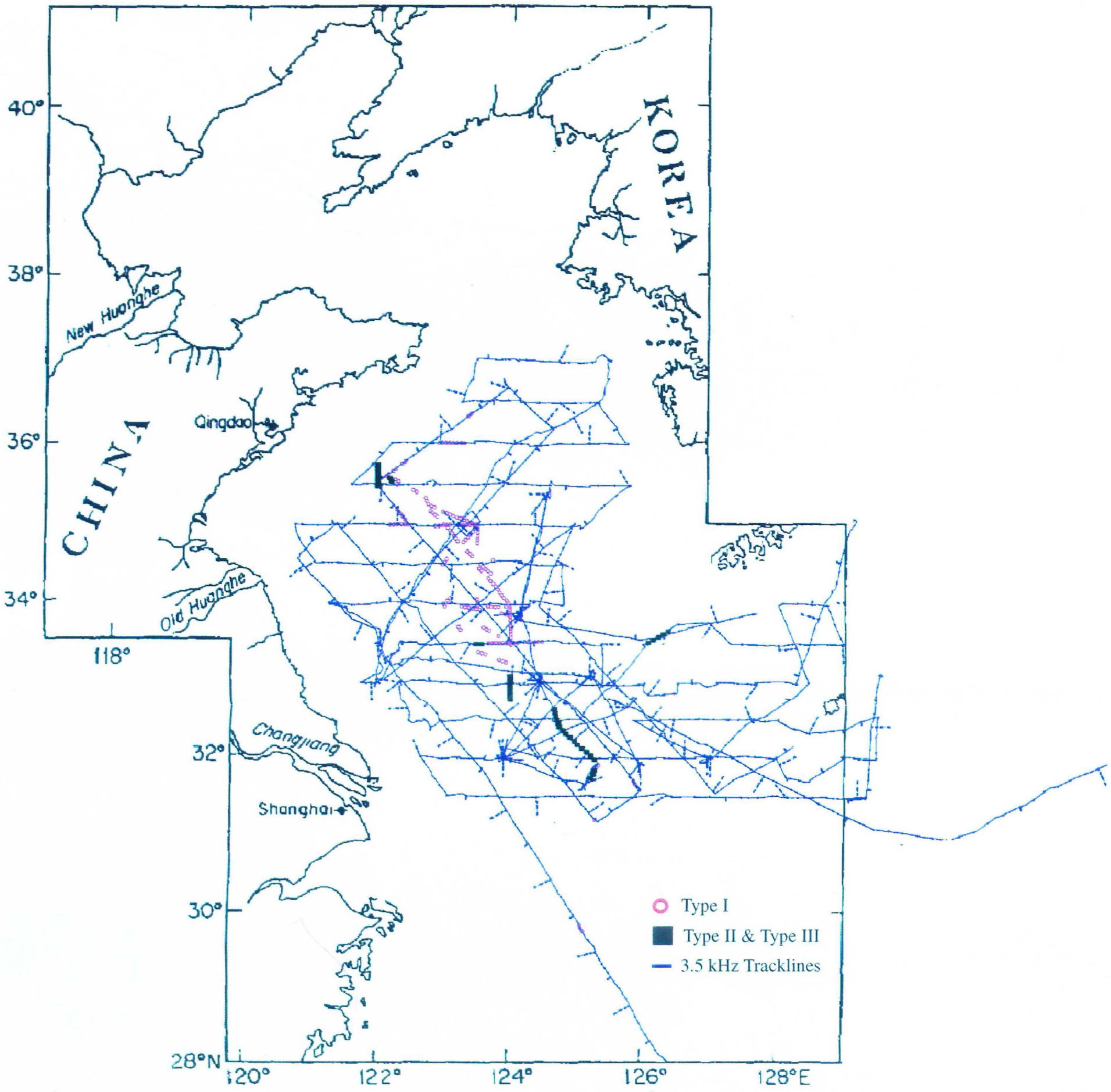

Figure 19. Distribution of types of 3.5 kHz subbottom records initially thought to be indicative of shallow buried gas.

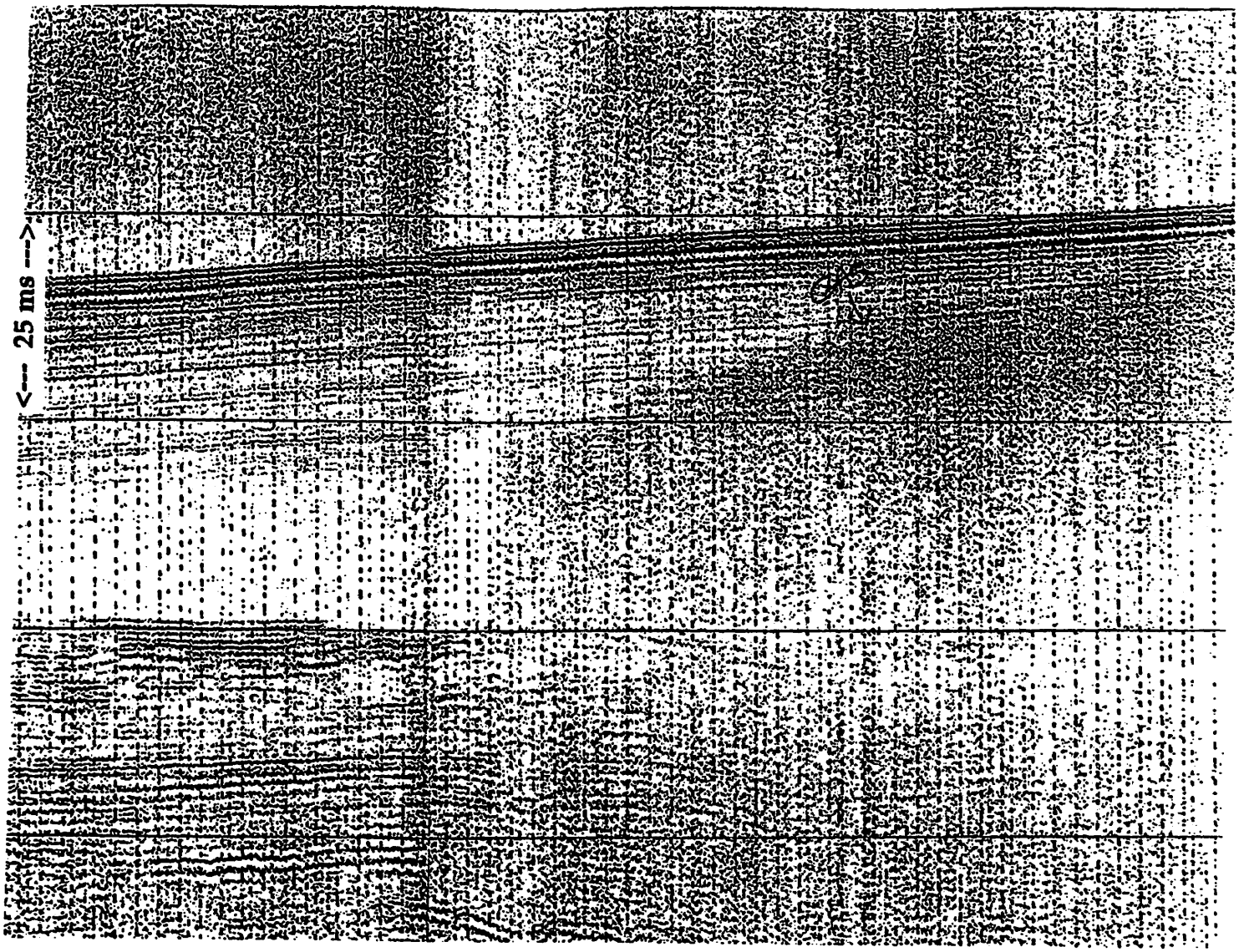

Figure 20. Geopulse profile showing buried gas on the Shandong mud wedge. See also Fig. 16 for another example.

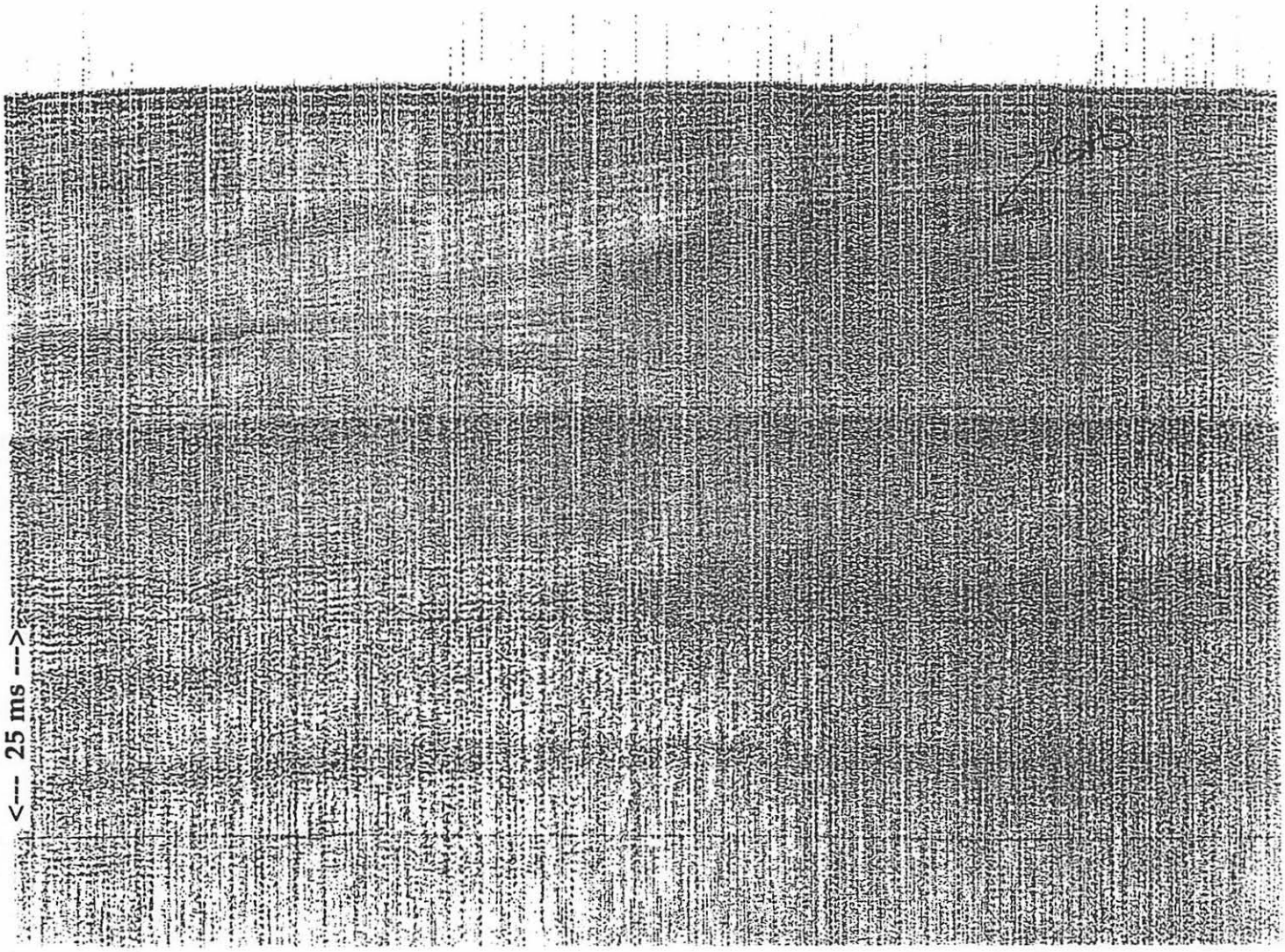

Figure 21. Geopulse profile showing buried gas on the Huanghe delta off the Jiangsu coast. Based on the few available high resolution seismic profiles, such examples of buried gas in this area are to be relatively few and scattered.

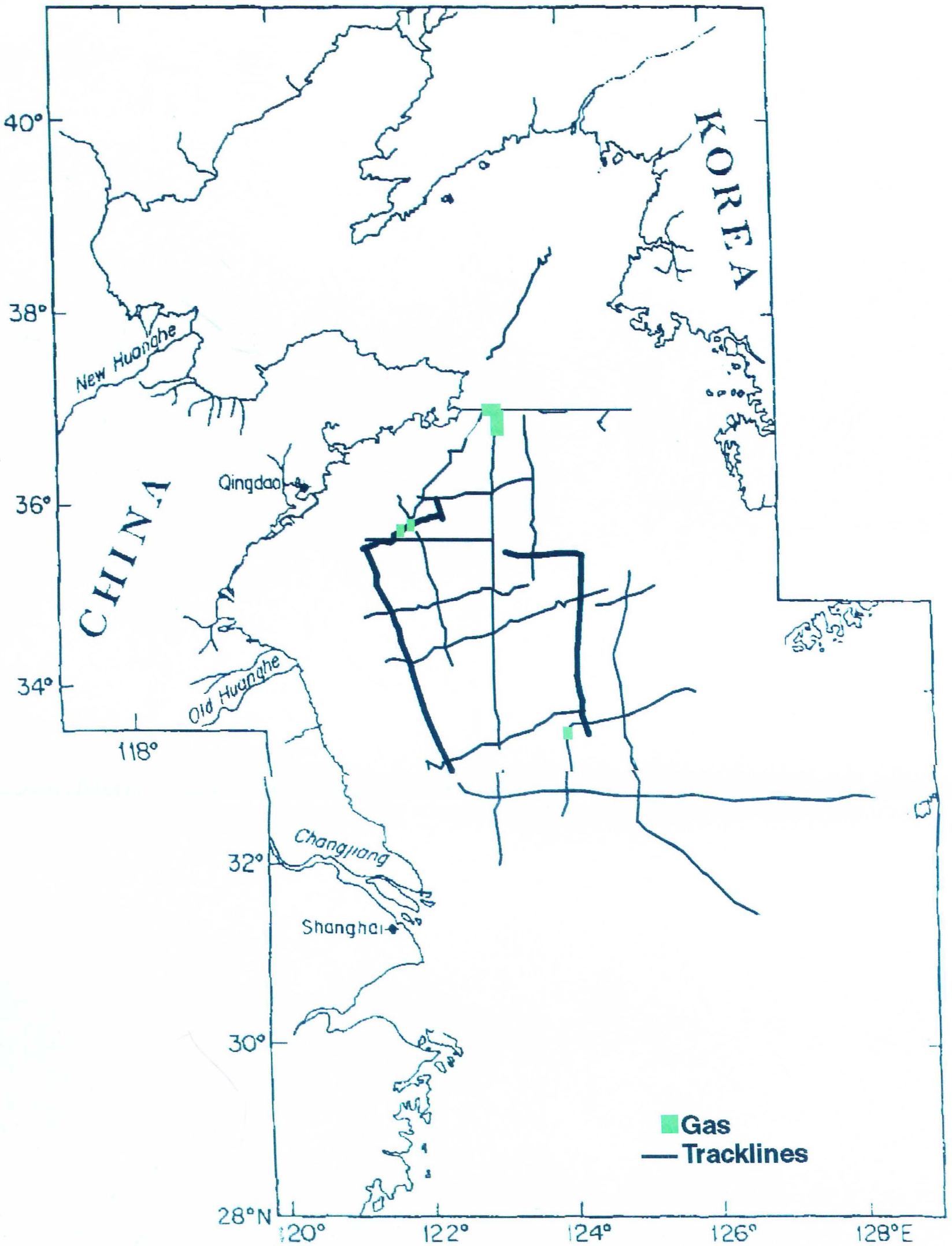

Figure 22. Distribution of shallow buried gas in the Yellow and East China Seas based on high-resolution seismic data.

The Neogene Record

Nature of the Deep Reflector. Deep seismic records show a very prominent reflector, so prominent that locally it can be seen at depths of 1 second beneath the sea surface, even though water depths locally are less than 100 msec (Fig. 23). The soft sediment throughout much of the study area explains the lack of multiples in the deeper seismic record, but the intensity of the deep reflector clearly indicates a great acoustic impedance, which also is noted in the internal multiples that this reflector sometimes displays (Fig. 23). We assume, therefore, a great difference in acoustic velocity between the overlying sediment and the reflector. Emery et al (1969; Wageman et al., 1970) assumed that this change from high velocity deep reflector and low-velocity shallow reflector was a discontinuity representing uplift of the Himalayas and subsequent rapid influx of terrigenous sediment; we agree with this interpretation, and our more extensive data base allows us to portray the thickness and structure in much greater detail.

Distribution of Sediments Overlying the Deep Reflector. The deep reflector is shallowest near the Shandong Peninsula and off all of western Korea, generally less than 25 ms (25 m assuming a mean velocity in the overlying sediments of 2000 m/sec) beneath the seafloor (Fig. 24). This structural high bows out from southwestern Korea, extending nearly half way across the East China Sea, clearly indicative of the Fukien-Reinan Massif (Fig. 4). Directly south of the Shandong Peninsula in the South Yellow Sea, in the eastern East China Sea south of Cheju Island, and along the northern slope of the Okinawa Trough, however, sediment thickness increases to more than 1-2 second (Figs. 24, 25). Given the increased water depths in the Okinawa Trough, the deep reflector locally lies more than 2 seconds beneath the sea surface (Figs. 26).

It also should be noted that these deeper seismic profiles also allow us the opportunity to denote the occurrence of faults, a few of which actually have surficial expression on the modern seafloor. With extremely few exceptions, faults in the Yellow and East China seas are restricted an E-W swath approximately 50 km wide, paralleling the Shandong Peninsula. A number of these faults have been high-lighted in Fig. 23. A much closer grid of seismic data, however, would be required to actually map this fault zone.

Geological Age and Significance of Sediments Overlying the Deep Reflector. Although the petroleum industry has drilled a relatively large number of deep holes in the study area, we have no direct core log data from these holes. Therefore it is difficult for us to specify the nature and age of the deep reflector and the overlying sediments. However, piecing together a number of geological maps available in the literature, some of which contain the results of deep boring logs, we can speculate on the nature and age of the sediment overlying the deep reflector. A collated map showing the thickness of Neogene sediments (Fig. 26) coincides very closely in configuration and total thickness to our map of the sediment overlying the deep reflector (Fig.

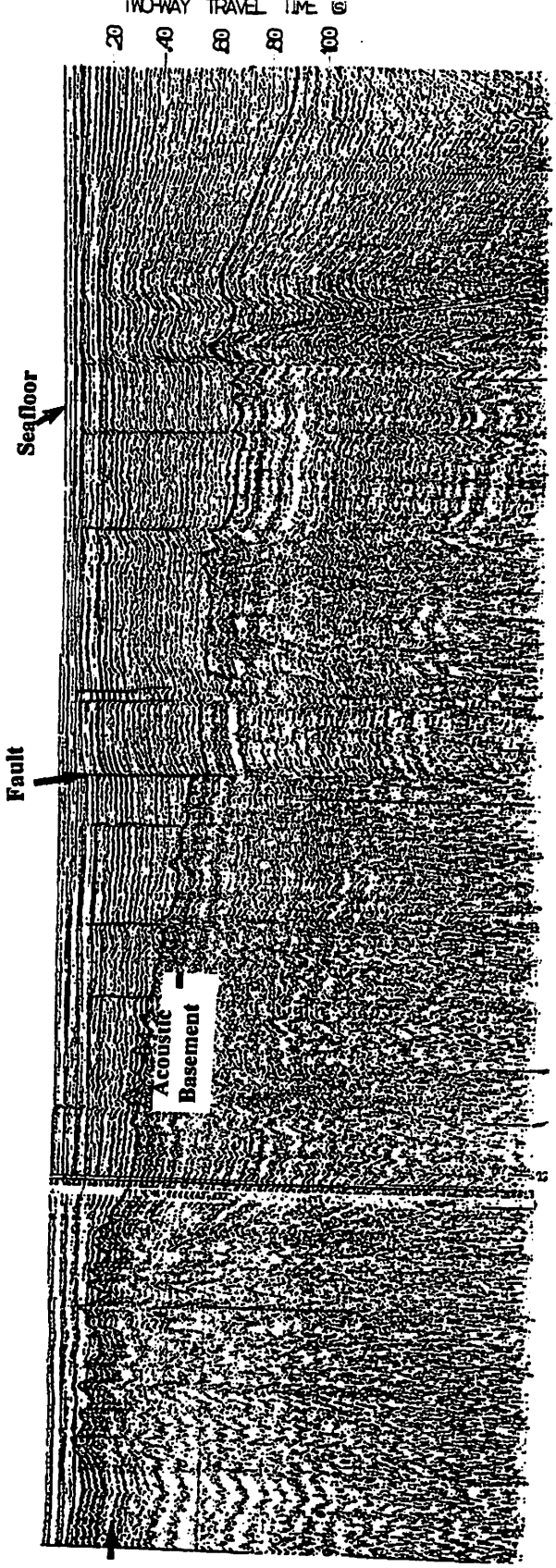

Figure 23. Single-channel multi-airgun profile in South Yellow Sea. Although water depth is only about 60 m (60 msec), the deep reflector can be seen nearly 1 sec beneath the seafloor, undoubtedly the result of acoustically soft overlying sediment and an acoustically hard deep reflector; note the internal multiples of the deep reflector. Prominent faults have been highlighted.

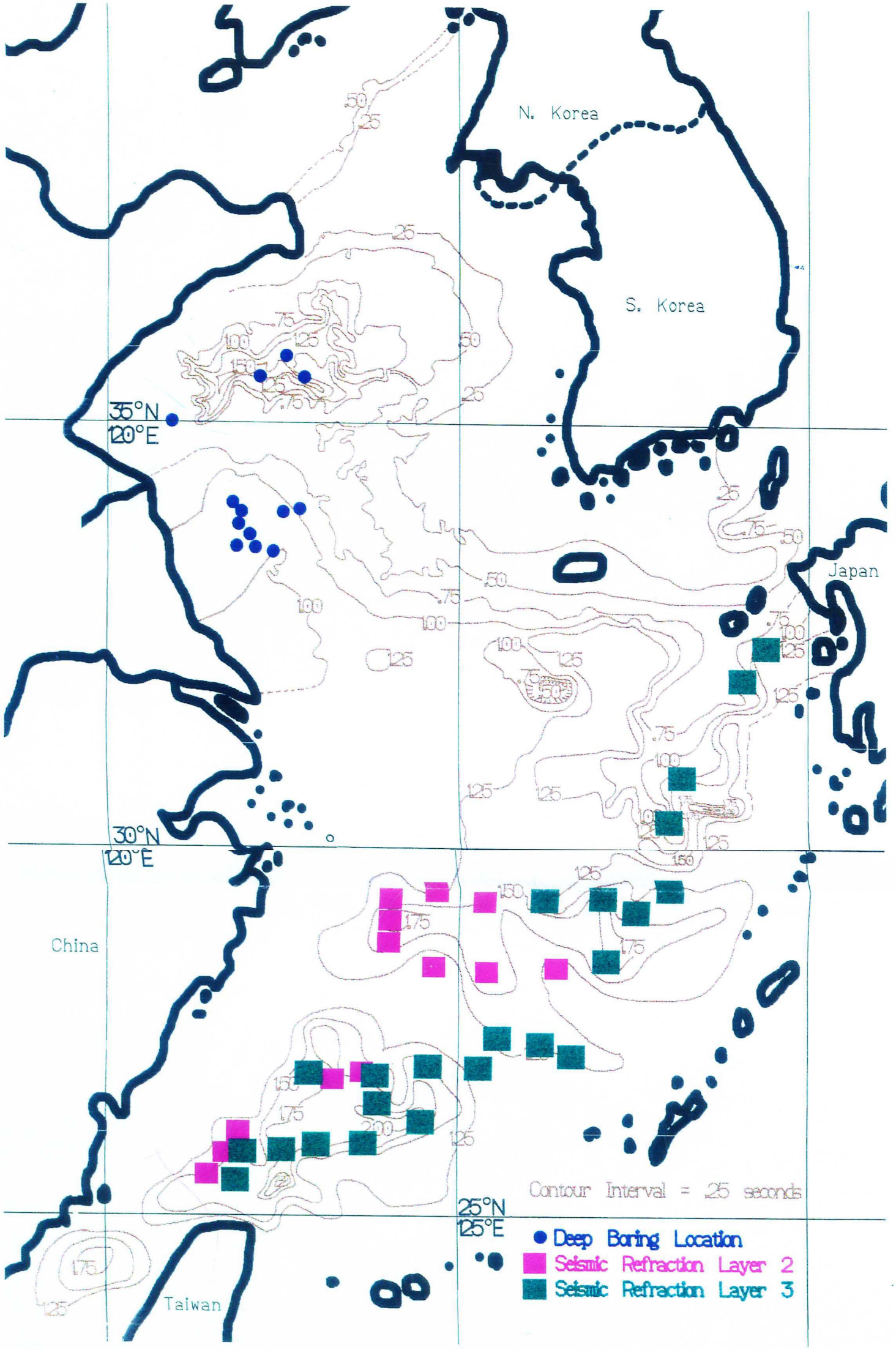

Figure 24. Isopach (in msec) of the sediment overlying the deep reflector. Based on analysis described in this paper, it is concluded that this sedimentary sequence is Neogene in age.

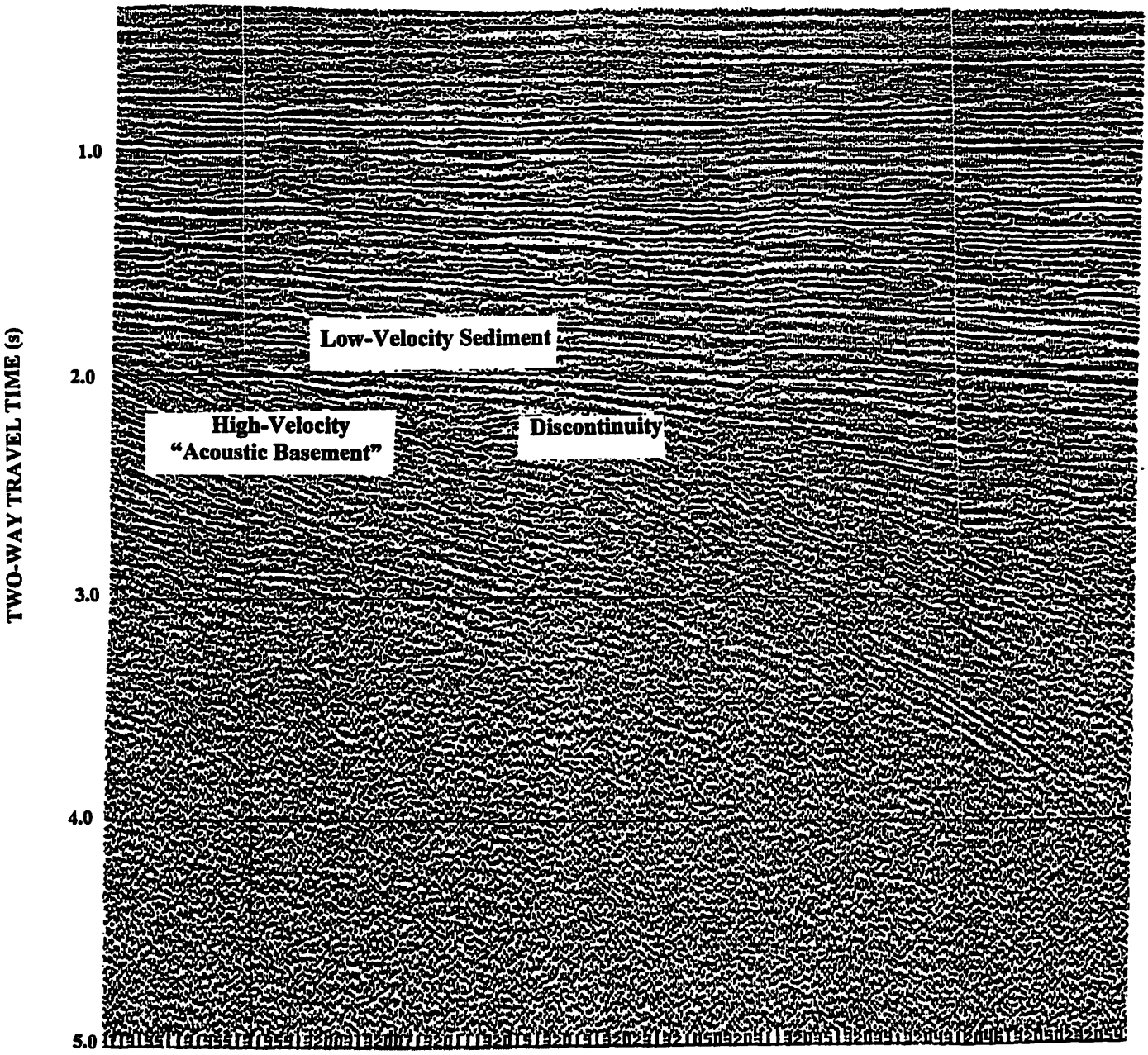

Figure 25. Deep multi-channel line in the southern East China Sea, obtained by Gulf Oil Company and given to the senior author by Chevron Oil Company. Note the horizontal sediments in the upper 2 seconds of the record and the seaward dipping deeper reflectors. The boundary between these two horizons is assumed to be the Neogene discontinuity.

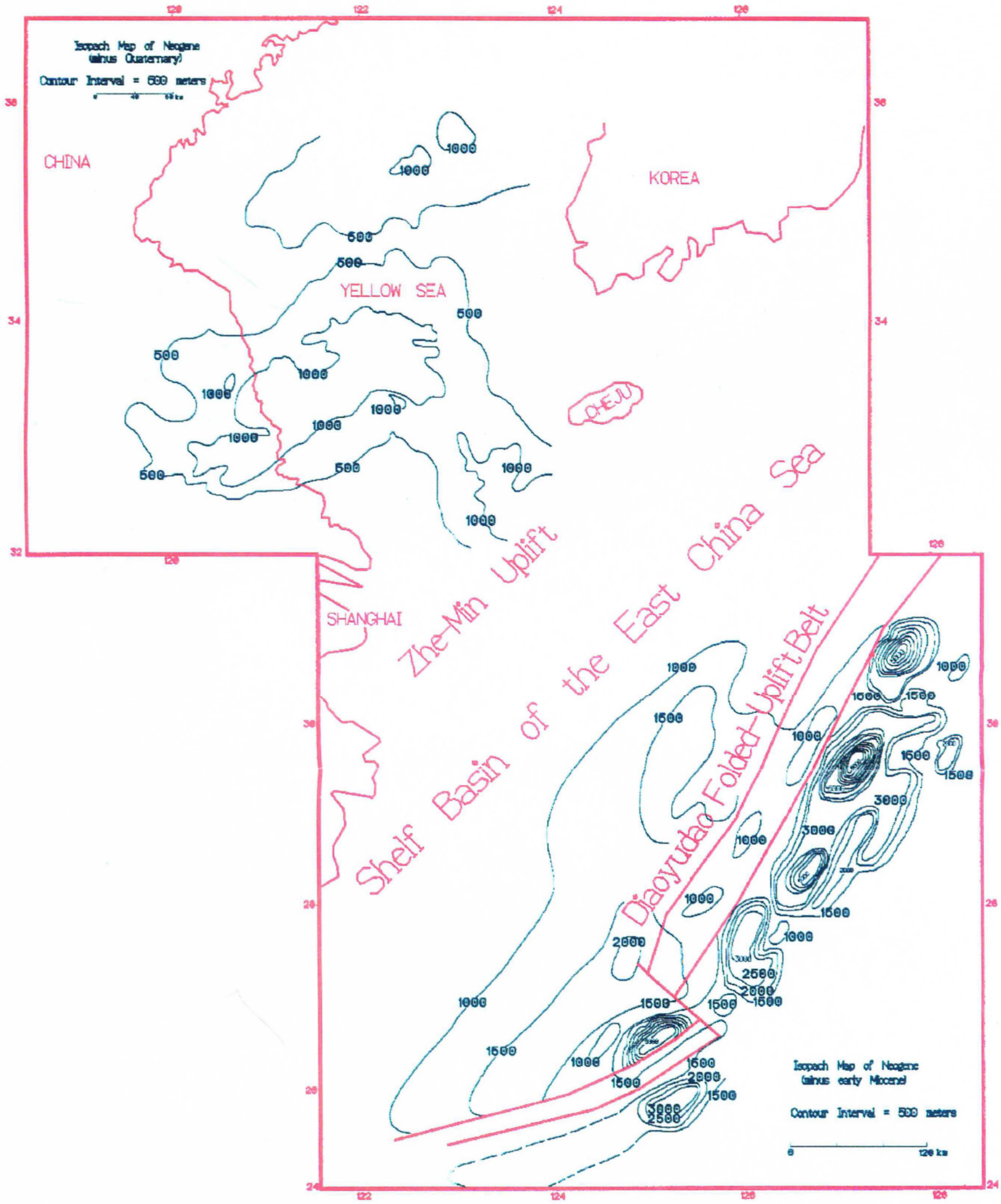

Figure 26. Collated map of several published maps (in Chinese and Japanese journals) showing thickness of the Neogene section in the Yellow and East China seas and surrounding land area. Note the close similarity between this map and Fig. 24.

24), leading us to conclude that this sediment section is Neogene in age. Although the collated map in Fig. 26 almost certainly is based of far more extensive and high-resolution data than our Fig. 24, it is given in meters, which we cannot easily convert into msec (assumed or termed velocities are not given in relevant Chinese or Japanese publications). Thus, for practical use, our maps are probably best used for shipboard purposes, where readings are in msec beneath the seafloor (Fig. 24) or sea surface (Fig. 27).[1]

Because we can find no well-log data describing the nature of the sediment in the layers overlying the deep reflector, we are forced to interpret seismic velocities, which unfortunately are not available for much of the study area (see above). Combining the seismic reflection and seismic refraction data, together with a basic knowledge of regional geology, we can piece together a general knowledge of the character of these sediment layers.

Beneath this upper layer of relatively low-velocity sediments is a layer with much higher velocity (3.0 to greater than 5.0 km/sec), which (because of the locally great change in acoustic velocities) we assume represents the deep reflector seen in our deep seismic reflection profiles. The thickness and depth of this overlying sediments agree closely with our sediment isopach and structure maps (Fig. 24). Judging from these velocities, we assume that this section is dominated by mudstones and unlithified sediments.

The correlation between our contoured maps and the layer 2-3, however, breaks down on the outermost East China Sea and Okinawa Trough, where our data indicate a much greater thickness that shown by the seismic refraction data (see, for example, Figs. 28, 29). This problem, however, is resolved if we assume that the lower part of this section is composed of higher velocity limestones (presumably reefal) rather than the mudstones seen shoreward. Lying over this lower limestone is the same mudstone seen in the shoreward seismic refraction sonobuoy stations.

[1] The northern-most seismic refraction profiles gathered by LDGO (Murauchi et al., 1968; Leyden et al., 1973; Ludwig et al., 1973) show that the upper layers of sediment overlying the deep have a velocity about 2.0 km/sec, whereas locally several higher velocity layers (2.4-2.6 km/sec, and 3.0 km/sec) also overlie the high-velocity reflector (Fig. 26). Lacking these velocity data, Emery et al. (1989) and Wageman et al. (1970) assumed an acoustic velocity of 2 km/sec for the entire Neogene section, which clearly (at least locally) is too low an average velocity. As a result, our Neogene maps are displayed in terms of seconds, rather than meters, of penetration.

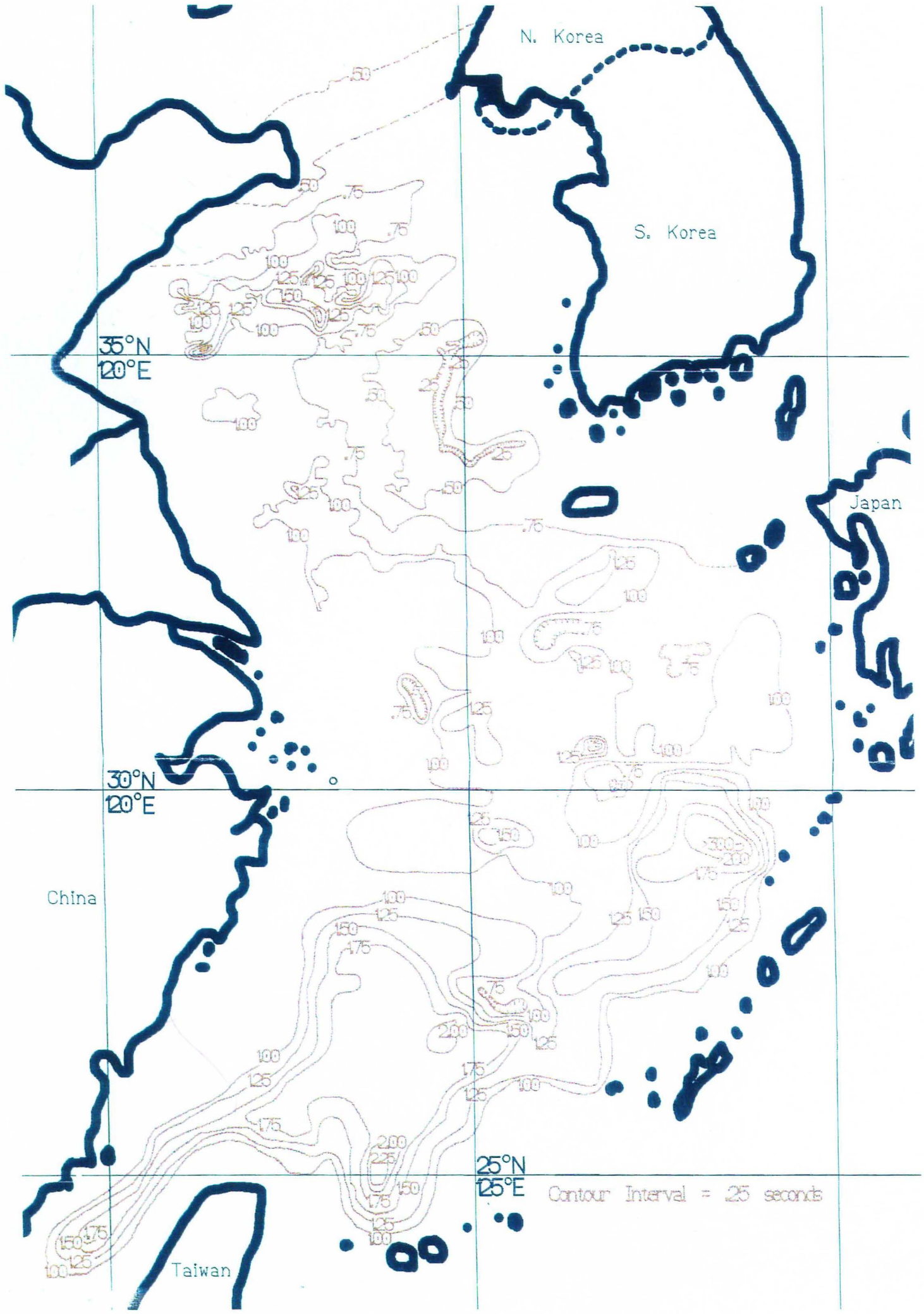

Figure 27. Structure map of the deep reflector. Reference level is sea level, in comparison with Fig. 24, where the reference level is the seafloor.

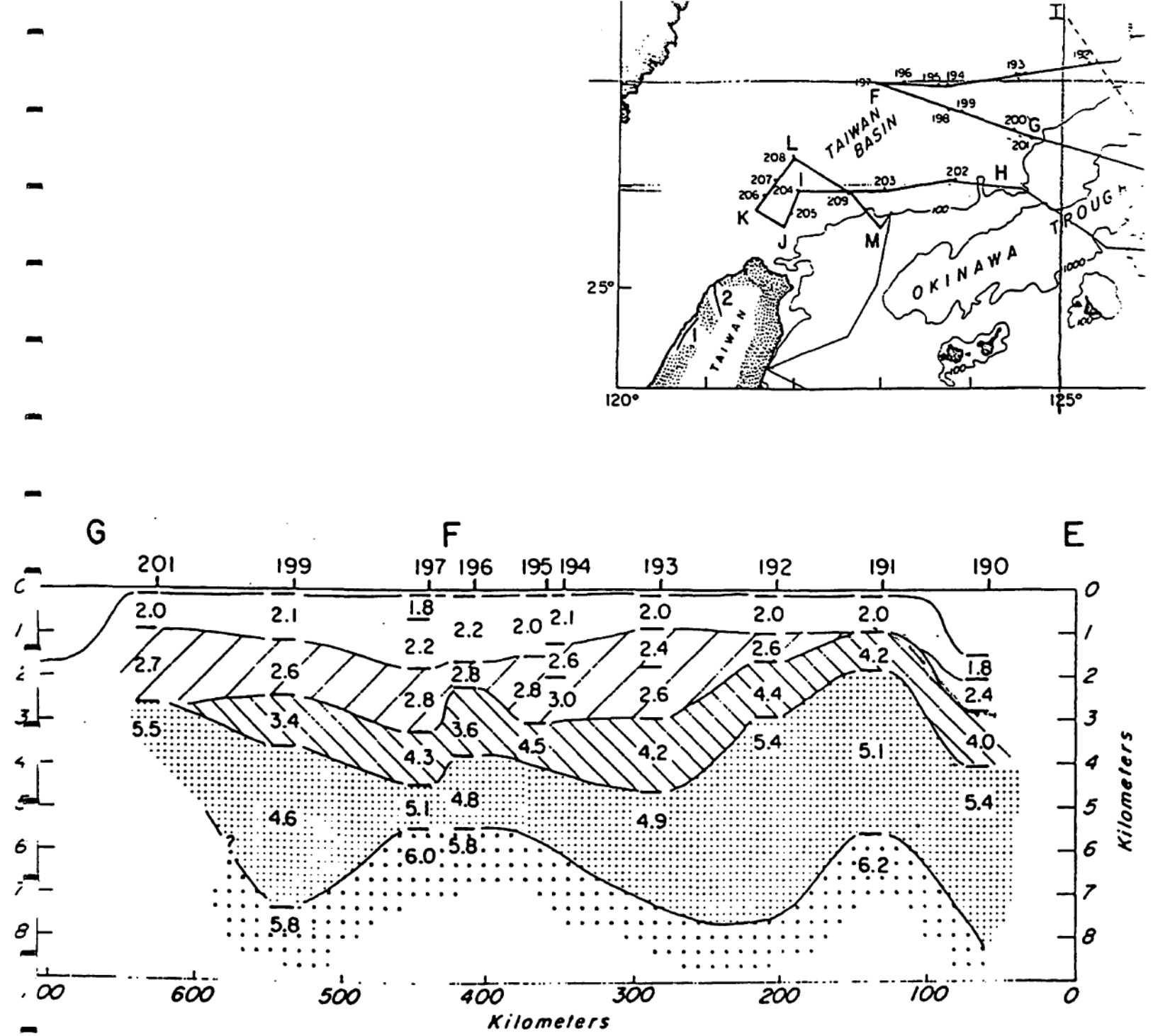

Figure 28. Interpreted seismic refraction profile from the southern East China Sea.. After Leyden et al. (1973).

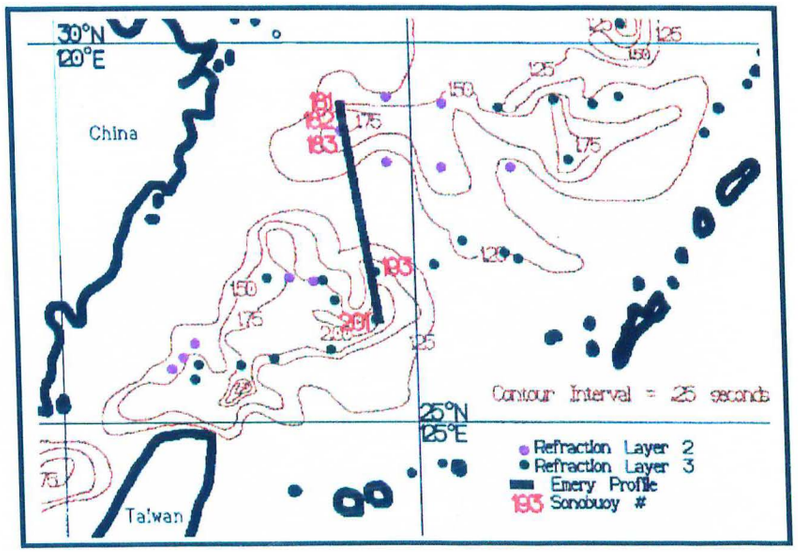

Figure 29. Interpreted seismic reflection profile (after Wageman et al., 1970) upon which interpreted seismic refraction sections (from Leyden et al., 1973) have been superimposed. Note that on the outer shelf one needs the high-velocity section to explain the entire Neogene section; it is thought that these high-velocity sediments represent early Miocene limestone, subsequently buried by terrestrial muds. Purple dots in the map indicate seismic refraction stations for which only layer 2 (velocities generally less than 3 km/sec) thicknesses are required to explain the Neogene section seen in the seismic reflection profiles. Dark green dots indicate seismic refraction stations for which layer 3 (velocities exceeding 4-5 km/sec) thicknesses are required to explain the entire Neogene section.

Having assumed something about the nature of the sediments, we can then speculate on the age of these sediments, although the close correlation between our sediment isopach and isopach maps digested from published data leaves little chance for doubt: The sediment overlying the deep reflector is Neogene in age, agreeing with the earlier assumption by Emery et al. (1969) and Wageman et al. (1970). As these earlier authors surmised and subsequent data have confirmed, collision of the Indian and Asian plates by the early Miocene elevated the Himalayas sufficiently that rivers draining these mountains experienced marked increases in their suspended loads.

Prior to the increased sediment discharge from mountainous rivers, much of the outer shelf along southern Asia was dominated by organic reefs; these were subsequently drowned as terrigenous discharge increased (e.g. Fulthorpe et al., 1989; Whiting et al., 1994). This shift from shelf-edge reefs to overlying mudstones would explain the marked shift in seismic velocities noted on the outer East China Sea shelf. In other words, this shift in velocities does not signify a sharp transition from older to younger rocks, but rather a change in sediment facies, from high-velocity early Miocene limestone to lower velocity mid- Miocene mudstone.

To summarize briefly, the sedimentary layer overlying the deep reflector is Neogene in age, its deposition resulting from the marked increase in sediment influx during the Eocene and early Miocene uplift of the Himalayas. Although seismic refraction data are few and restricted to the outermost East China Sea and adjacent Okinawa Trough, correlation with seismic reflection profiles suggest that the lower Neogene on the inner and mid shelf is predominantly mudstone (seismic velocities of 2.0 to 2.5 km/sec), whereas the outer shelf lower Neogene consists of reefal limestones (seismic velocities of 3.0 to as much as 5.0 km/sec). Presumably the limestone facies was drowned some time in the early to mid-Miocene, as the Himalayas continued to uplift and the terrigenous sediments spread out across the entire shelf.

Unknowns and Future Studies

The rather extensive geophysical data base (Fig. 2) provides us with an excellent regional understanding of the morphology, sediment distribution and Neogene structure and history of the Yellow and East China seas. On a more local basis, however, the data base is less sufficient, and there are a number of parameters that have been delineated only in scattered areas. For example, to date we have no seismic refraction data from the Yellow Sea, and, in fact, no data from the East China Sea north of about 30° N.

Moreover, despite their abundance, the NAVO 3.5 kHz data were recorded at 1 second sweeps (only analog records exist), thereby not allowing us to be able to resolve 5-20 msec features that define the Holocene record; as a result, the NAVO 3.5 kHz profiles have little use in defining the surficial or Holocene geology. The NAVO sparker data, while providing excellent high-resolution seismic profiles of the upper 300-500 msec of the sedimentary section, had too weak a seismic source to achieve deeper penetration. As a result, there are many areas for which we have insufficient deeper seismic data.

The seismic data base off Korea, for example, is much less complete that it is off China. In large part that results from the fact that the senior author of this report has worked for many years with the Chinese, thus allowing him access to Chinese coastal waters as well as more detailed work in areas of particular interest. For obvious reasons we have no data off North Korea, even though the marine geology in this area may have particular naval relevance in terms of surficial sediments and morphology (e.g., the submarine sand dunes off the Yalu River). Whereas much of the seafloor in the western and central portions of the Yellow and East China seas is featureless (except for the ubiquitous trawl marks), the western Korean shelf contains many sedimentary ridges, some of whom may represent relict features formed during lower sea level. Swath-mapping would be particularly useful in such areas, particularly if it could be done in conjunction with high-resolution seismic profiling.

Finally, ground-truth data are equally difficult to obtain. For example, we know little about the geotechnical properties of the surficial sediments in the area. The early work by Butenko et al. (1985) and Keller and Ye (1985) has not been (to the best of the present writers' knowledge) updated or expanded upon. Huanghe-derived sediments, for example, because they contain higher concentrations of silt, presumably also contain more porewater, and thus are less able to support bottom-mounted objects.

We also lack access to any drill logs from deep borings in the area. We have accessed some interpreted profiles from the literature, although these logs generally show only depth to a certain horizon; luckily for this report, the Neogene seems to be one horizon in which the Chinese scientists have placed particular interest. While we have surmised Neogene facies from limited seismic refraction data, however, we have no way of knowing if these assumptions are correct. In this respect also, logs from deep borings would prove useful.

References Cited

Butenko, J., Milliman, J.D., and Ye, Y.C., 1985. Geomorphology, shallow structure, and geological hazards in the East China Sea. *Cont. Shelf Res.*, 4, 121-141.

Chen, Y.G., Peng, G., and Jiao, W.G., 1985. Radiocarbon dates from the East China Sea and the geological implications. *Quat. Res.*, 24, 197-203.

DeMaster, D.J., McKee, B.A., Nittrouer, C.A., Qian, J.C., and Cheng, G.D., 1985. Rates of sediment accumulation and particle reworking based on radiochemical measurements from continental shelf deposits in the East China Sea. *Cont. Shelf Res.*, 4, 143-158.

Emery, K.O., Niino, H. and Sullivan, B., 1971, Post-Pleistocene levels of the East China Sea. in K.K. Turekian (ed.), *Late Cenozoic Glacial Ages*, Yale Univ. Press, New Haven, 381-390.

Emery, K.O. et al., 1969. Geological Structure and some water characteristics of the East China Sea and Yellow Sea. *U.N. ECAFE, Comm. Coord. Joint Prospecting for Mineral Resources in Asia Offshore Areas*, Tech. Bull., 2, 3-43.

Jeong, K.S., Hand, S.J. and Suk, B.C., 1984. A sedimentological study in the southeastern Yellow Sea. in Marine Geology and Physical Processes of the Yellow Sea, Proc. Korea-U.S. Seminar and Workshop, Korea Inst. Energy and Resources, 96-116.

Keller, G.H. and Ye, Y.C., 1985. Geotechnical properties of surface and near-surface deposits in the East China Sea. *Cont. Shelf Res.*, 4, 159-174.

Leyden, R., Ewing, M., and Murauchi, S., 1973. Sonobuoy refraction measurements in East China Sea. *Amer. Assoc. Petrol. Geol. Bull.*, 57, 2396-2403.

Ludwick, W.J. et al., 1973. Structure of East China Sea - West Philippine Sea margin off southern Kyushu, Japan. *J. Geophys. Res.*, 78, 2526-2536.

Milliman, J.D., Qin, Y.S., and Park, Y.A., 1989. Sediments and sedimentary processes in the Yellow and East China seas. in A. Taira and F. Masuda (eds.), *Sedimentary Facies in the Active Plate Margin*. Terra Sci. Publ., Tokyo, 233-249.

Milliman, J.D., Qin, Y.S., Ren, M.E., and Saito, Y., 1987. Man's influence on the erosion and transport of sediment by Asian rivers: The Yellow River (Huanghe) example. *J. Geol.*, 95, 751-762.

Murauchi, S. et al., 1968. Crustal structure of the Philippine Sea. *J. Geophys. Res.*, 73, 3143-3171.

Niino, H. and Emery, K.O., 1961. Sediments of shallow portions of East China Sea and South China Sea. *Geol. Soc. Amer. Bull.*, 72, 731-762.

Qin, Y.S. and Li, F., 1983. Study of influence of sediment loads discharged from Haunghe River on sedimentation in Bohai Sea and Huanghai Sea. in *Proceedings of the International Symposium on Sedimentation on the Continental Shelf with Special Reference to East China Sea.* China Ocean Press, Beijing, 83-92.

Wageman, JAM., Hilde, T.W.C., and Emery, K.O., 1970. Structural framework of East China Sea and Yellow Sea. *Amer. Assoc. Petrol. Geol. Bull.*, 54, 1611-1643.

Wang, J.T. and Wang, P.X., 1982. Relationship between sea-level changes and climatic fluctuation in East China since late Pleistocene (in Japanese). *Quat. Res.*, 21, 101-114.

Whiting, B.M., Karner, G.D. and Driscoll, N.W., 1994. *J. Geophys. Res., 99,* 13791.

Wang, Z., 1982., Study on the origin and characteristics of relict sands in the western South Yellow Sea. *Marine Geol, Quat. Geol.*, 6, 63-70.

Yanagida, M. and Kaizuka, S., 1982. Recent Chinese studies on the sea level change since the last interglacial in the Sea of Bohai, Yellow Sea and East China Sea (in Japanese). *Quat. Res.*, 21, 115-122.